


Image Cover Sheet

CLASSIFICATION UNCLASSIFIED	SYSTEM NUMBER 143924 
---	--

TITLE
A PROOF OF CONCEPT IMPLEMENTATION OF AN FFT-BASED EXCISOR

System Number:
Patron Number:
Requester:

Notes:

DSIS Use only:
Deliver to: DK



National
Defence

Défense
nationale



A PROOF OF CONCEPT IMPLEMENTATION OF AN FFT-BASED EXCISOR

by

Brian Kozminchuk

DEFENCE RESEARCH ESTABLISHMENT OTTAWA
TECHNICAL NOTE 93-16

Canada

September 1993
Ottawa



National
Defence

Défense
nationale

A PROOF OF CONCEPT IMPLEMENTATION OF AN FFT-BASED EXCISOR

by

Brian Kozminchuk

*Communications Electronic Warfare Section
Electronic Warfare Division*

DEFENCE RESEARCH ESTABLISHMENT OTTAWA
TECHNICAL NOTE 93-16

PCN
041LK

September 1993
Ottawa

ABSTRACT

An FFT-based algorithm for suppressing narrowband interference in direct sequence spread spectrum signals has been implemented across three TMS320C30 processors forming part of the Advanced Communications Electronic Support Measures System (ACES). An FFT approach is especially attractive because of its computational economy. The basic problem to be solved is described, followed by a description of the algorithm. This technique is feasible so long as the bandwidth of the interference during the observation time over which the FFT is calculated is much less than the bandwidth of the spread spectrum signal. One of the laborious aspects of implementing this algorithm (and perhaps any others to be implemented on ACES at a later date) was to efficiently distribute the workload across the three TMS320C30 processors so as to achieve real-time performance; this objective was achieved, although the spread spectrum bandwidths which could be processed were not high. The experience gained will demand the incorporation of efficient ways of reducing the development/testing cycle in the ACES system when attempting to implement algorithms for any signal processing application.

RÉSUMÉ

La suppression d'interférences à bande passante étroite dans des signaux à spectre étalé par des séquences directes a été réalisée par un algorithme utilisant une FFT. Il fut mis en oeuvre grâce à trois processeurs TMS320C30 qui font partie d'un système de mesures de soutien électroniques pour communications perfectionnées appelé ACES. Cette technique utilise une FFT et est particulièrement intéressante parce qu'elle requiert peu de calculs. Un problème typique ainsi que l'algorithme sont décrits. Il est possible d'utiliser cette technique si la bande passante de l'interférence pendant le temps d'observation utilisé pour calculer la FFT est beaucoup plus petite que la bande passante du signal à spectre étalé. Une des difficultés rencontrées lors de la mise en oeuvre de cet algorithme (et peut-être aussi pour d'autres algorithmes d'ACES) fut de distribuer efficacement les tâches aux trois processeurs TMS320C30 de façon à permettre le fonctionnement en temps réel. Cet objectif fut atteint bien que pour des bandes passantes limitées du signal à spectre étalé. Nous avons aussi établi l'importance de trouver des façons efficaces de réduire la durée du processus de développement et de vérification lors de la mise en oeuvre d'algorithme de traitement de signaux pour ACES.

EXECUTIVE SUMMARY

This technical note presents the experimental results of an FFT-based technique for filtering narrowband interference from spread spectrum communications signals. This algorithm has been implemented across three TMS320C30 processors forming part of the ACES system.

Spread spectrum signals are used extensively in military communication systems. The technique described herein applies equally to both Electronic Support Measures (ESM) systems and direct sequence spread spectrum communication systems. In the former application, the ESM system may be attempting to intercept the spread spectrum signal, but the narrowband interference may be hampering this effort. In the latter application, the spread spectrum communication system may require additional assistance to suppress the interference. Since the open literature has been devoted to this latter case, the material presented here focuses on this application.

One of the attributes of direct sequence spread spectrum communication systems is their ability to combat interference or intentional jamming by virtue of the system's processing gain inherent in the spreading and despreading process. The interference can be attenuated by a factor up to this processing gain. In some cases the gain is insufficient to effectively suppress the interferer, leading to a significant degradation in system performance as manifested by a sudden increase in bit error rate. If the ratio of interference bandwidth to spread spectrum bandwidth is small, the interference can be filtered out to enhance system performance. However, this is at the expense of introducing some distortion onto the signal. This process of filtering is sometimes referred to as interference excision.

The FFT implementation described herein is especially attractive because of its computational economy. The algorithm consists of power spectrum estimation using an FFT-based routine, interpolation of the power spectrum at a set of equally-spaced points different from those calculated by the FFT, and design of an FIR linear phase filter which filters the data, i.e., suppresses the interference. This technique is feasible so long as the bandwidth of the interference during the observation time over which the FFT is calculated is much less than the bandwidth of the spread spectrum signal.

There are two salient points from this work. The first is the high degree of effort that was required to implement an algorithm in a multi-processor environment which implies that efficient ways of reducing the development/testing cycle will have to be incorporated into the ACES system. Even with the effort that was required to implement this excision application, the overall bandwidth of the spread spectrum signal

had to be scaled down significantly so as to be able to demonstrate a real-time interference suppression capability. It should be noted too that even with scaling down the frequencies of operation, the despreading had to be done off-line.

The second point is the need for high quality digital receivers and several more processors. The additional processors will have to be configured in such a way so as to provide flexibility in interprocessor communications as well as the capability to handle significantly higher data transfer rates. These requirements will allow for an increase in the signal bandwidth which can be processed. A system currently being developed which will meet these requirements includes a Steinbrecher digital receiver, Austek FFT processors and a nine cell iWarp array.

ACKNOWLEDGEMENTS

The author would like to express his gratitude to Mr. Hugh Parliament of Applied Silicon Inc. Canada for the software he wrote and the data he collected during the course of this work.

TABLE OF CONTENTS

ACKNOWLEDGEMENTS	iii
ABSTRACT/RÉSUMÉ	iii
EXECUTIVE SUMMARY	v
TABLE OF CONTENTS	vii
LIST OF TABLES	ix
LIST OF FIGURES	xi
1.0 INTRODUCTION	1
2.0 PROBLEM DESCRIPTION	2
3.0 COMMUNICATIONS MODEL	3
4.0 EXCISION FILTER ALGORITHM	7
5.0 EXPERIMENTAL SET-UP	8
6.0 EXPERIMENTAL RESULTS	13
7.0 CONCLUSIONS	29
REFERENCESREF-1

LIST OF TABLES

Table 1: Excision Filter Algorithm.	9
Table 2: Spread Spectrum Signal Parameters.	11

LIST OF FIGURES

Figure 1: Spread Spectrum Signal of Bandwidth B_{ss} and Narrowband Jammer of Bandwidth B_j	3
Figure 2: Two conceptual approaches to interference excision for BPSK signals: (a) Analog excisor; (b) Digital excisor.	4
Figure 3: Spread spectrum communications model.	5
Figure 4: Sampled spread spectrum signal and noise at the output of the analog bandpass filter H_{bp} of bandwidth B_{bp}	7
Figure 5: Experimental setup for excision experiments.	10
Figure 6: DAR 4000 and VMEC30 sub-systems of Fig. 5.	12
Figure 7: Several frames of system digital noise at the output of the DAR 4000.	14
Figure 8: Power spectral densities of system noise and additive noise plus system noise before decimation; the abscissa has been normalized by $f_s = 125$ kHz.	15
Figure 9: Power spectral densities of system noise and additive noise plus system noise after decimation.	16
Figure 10: Several frames of the unspread data sequence at the output of the DAR 4000. The number of samples per bit is 80 (i.e., 8 samples/chip).	17
Figure 11: Power spectral density of unspread data sequence at the output of the DAR 4000.	18
Figure 12: Two frames of the PN sequence at the output of the DAR 4000 with a sampling rate of 8 samples/chip.	19
Figure 13: What the two frames of the PN sequence code in Fig. 12 would look like if they had been applied to a digital version of an integrate-and-dump system operating at the chip rate.	20
Figure 14: Power spectral density of a block of samples of the spreading sequence at the output of the DAR 4000.	21
Figure 15: Power spectral density of a block of samples of the spread spectrum signal at the output of the DAR 4000.	22

- Figure 16: An example of the tone interference (located at 0.024 Hz) plus system noise in the time domain (upper frame) and frequency domain (lower frame) at the output of the DAR 4000. 23
- Figure 17: Signal, noise and tone interference (located at 0.024 Hz) in the time domain (upper frame) and frequency domain (lower frame) at the output of the DAR 4000; $E_b/N_0 = 5$ dB, interference-to-signal ratio equal to 20 dB. 24
- Figure 18: Power spectra of signal plus tone interference located at 8×10^{-5} Hz (upper frame) and 0.024 Hz (lower frame) at the output of the DAR 4000; interference-to-signal ratio equal to 10 dB. Additive noise was not present. 25
- Figure 19: Power spectrum of signal, noise and tone interference (located at 0.024 Hz) in the time domain after decimation by 8 in the VMEC30 board; $E_b/N_0 = 5$ dB, interference-to-signal ratio equal to 20 dB. 26
- Figure 20: Several notch filter frequency responses as calculated by the VMEC30 processor based on a tone with system noise only (no additive noise). Each frequency response curve was calculated from a block size of 512 and subblock size of 32. The filter order was 31, the sampling rate was decimated by a factor of 8 (i.e., $125/8 = 15.625$ kHz), and the tone frequency was located at 3 kHz (normalized frequency of 0.192 Hz). 27
- Figure 21: Effect of the excision filter. The two power spectra shown were each calculated from a block of 8192 points using the Welch algorithm, with sub-blocks of 512 points, no overlapping, and a rectangular window. The excision filter coefficients were calculated from block sizes of 512 points and sub-block sizes of 32 points. The filter order was 31, the sampling rate was decimated by a factor of 8 (i.e., $125/8 = 15.625$ kHz), and the tone frequency was located at 3 kHz (normalized frequency of 0.192 Hz). 28
- Figure 22: Theoretical and experimental bit error rate curves based on signal-to-noise ratios calculated at the output of the DAR 4000. No interference was present. 31
- Figure 23: Theoretical and experimental bit error rate curves for single-tone interference located at frequencies f_i of 10 Hz and 3 kHz offset from the carrier. The signal-to-noise and interference-to-signal ratios were calculated at the output of the DAR 4000. 32

Figure 24: Theoretical and experimental bit error rate curves for single-tone interference located at frequencies f_i of 10 Hz and 3 kHz offset from the carrier. The signal-to-noise and interference-to-signal ratios were calculated at the output of the DAR 4000. 33

1.0 INTRODUCTION

Direct sequence spread spectrum communication systems have an inherent processing gain which can reduce the effects of jammers or unintentional interference. When these intruding signals have a power advantage over the spread spectrum system, a severe degradation in communications results. However, communications can be enhanced somewhat by filtering the interference, particularly if its bandwidth is significantly less than the bandwidth of the spread spectrum signal.

A host of digital filtering algorithms have been developed over the years to address this problem [1, 2, 3, 4, 5]. The received signal, noise and interference are applied, for example, to a filter matched to a chip and the output is sampled at the chip rate. One approach is to assume that the resulting sampled data can be modelled as an autoregressive (AR) process. In this case, the AR coefficients or their related lattice reflection coefficients can be determined from the maximum entropy algorithm [6], stochastic gradient algorithms [7], or block and recursive least squares algorithms [8, 9]. Estimates of these coefficients by the above algorithms lead directly to transversal or lattice filter structures, both of which act as whitening filters for the assumed AR process. This approach to suppressing interference (or excision as it is sometimes referred to) is possible because of the non-coherency of the signal and noise samples, and the more coherent interference samples resulting from the latter's narrowband nature.

The focus of this technical note is to present experimental results of an FFT-based technique applied to interference suppression in direct sequence spread spectrum communications signals. This technique first appeared in [2] and was further elaborated upon in [10].

The FFT approach is of practical importance because of the processing speed afforded by the FFT algorithm compared to the direct calculation of the discrete Fourier transform (DFT) for high filter orders, and the existence of high-speed DSP hardware currently available to calculate the FFT. This latter approach has been implemented as a proof-of-concept in the Advanced Communications Electronic Support Measures System (ACES) [11] using the TMS320C30¹ hardware therein. This technique will also be implemented on the high-speed iWarp² processors which also form part of the ACES system.

The purpose of this technical note is to present the experimental results of the FFT-based approach as implemented in the ACES system using its embedded TMS320C30

¹This is a Texas Instruments digital signal processing chip.

²This is an Intel product.

processors. The following topics will be covered:

- a description of the problem to be solved
- the communications model used in the experiments
- the algorithm which calculates the filter coefficients of the suppression filter
- a description of the experimental set-up
- experimental results, and
- concluding remarks.

2.0 PROBLEM DESCRIPTION

The basic problem is illustrated in Fig. 1. Consider the received spread spectrum signal of bandwidth $B_{ss} = 2R_c$, centered at an intermediate frequency (IF) of f_0 Hz, where R_c is the chip rate of the spread spectrum signal. Also present in the signal bandwidth is an interferer of bandwidth $B_i \ll B_{ss}$, and centered at $f_0 + \delta f$. The interference can be filtered out either at the IF or at baseband. There are several possible configurations which can effect this filtering. Two concepts are illustrated in Figs. 2(a) and (b), which will not necessarily produce equivalent results because of the way in which the excision filters are implemented, i.e., whether or not an optimum criterion is being met. In these figures $u(t)$ is defined as

$$u(t) = s(t) + n(t) + i(t), \quad (1)$$

where $s(t)$ is the spread spectrum signal, $n(t)$ is bandpass Gaussian noise and $i(t)$ is the narrowband interfering signal.

In Fig. 2(a), $u(t)$ is applied to an excision filter first. The output is despread by correlating it with the pseudo-noise (PN) sequence. The despread signal is then mixed down to baseband and the resulting signal is bit-detected.

In Fig. 2(b), $u(t)$ is mixed down to baseband and then sampled at the chip rate.³ The assumption is made that carrier and chip synchronization have been achieved, which will not be the case initially. The sampled sequence, u_n , is processed by an algorithm which determines a set of filter coefficients for the excision filter; an optimization criterion which depends on the algorithm can be used. For example, the autoregressive approach alluded to in the introduction bases its design on the minimization of the mean-squared

³One can also bandpass sample, which is the approach taken in the experiments reported on herein.

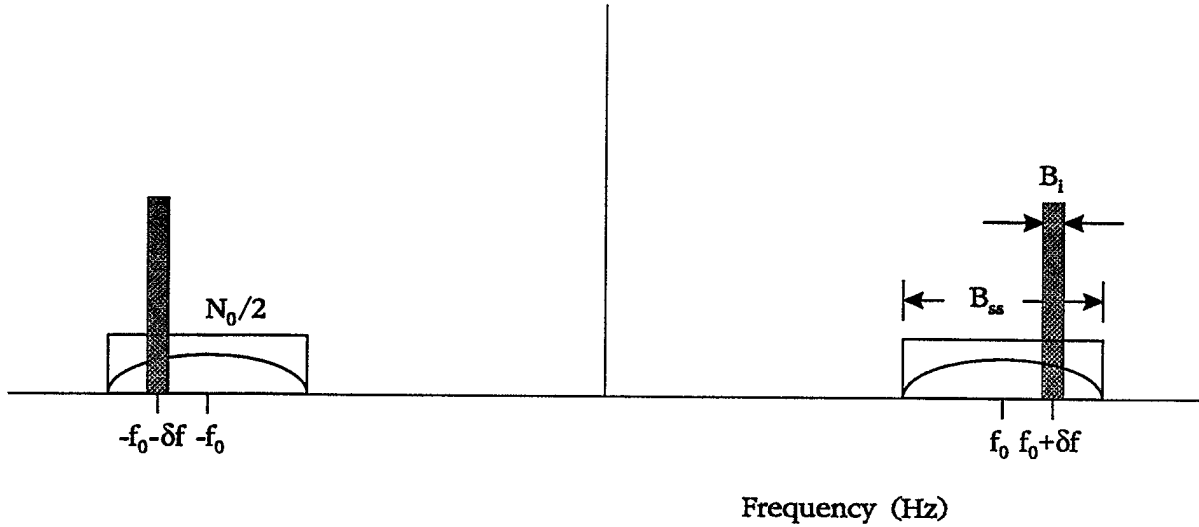


Figure 1: Spread Spectrum Signal of Bandwidth B_{ss} and Narrowband Jammer of Bandwidth B_i .

value of a prediction error, e_n . The FFT approach considered in this report does not apply any optimization criterion *per se* since the filter design is determined from the reciprocal of the estimated power spectrum.

In either approach that is used to calculate the filter coefficients, the filter's output signal e_n is applied to the PN correlator followed by a bit detector.

3.0 COMMUNICATIONS MODEL

The basic elements of a direct sequence spread spectrum system used in the experiments are shown in Fig. 3. The received waveform $r(t)$, consisting of a spread spectrum signal, additive white Gaussian noise, and narrowband interference is applied to a bandpass filter $H_{bp}(f)$ of bandwidth B_{bp} , whose output was defined in Eq. 1. In Eq. 1, the spread spectrum signal is generally defined as

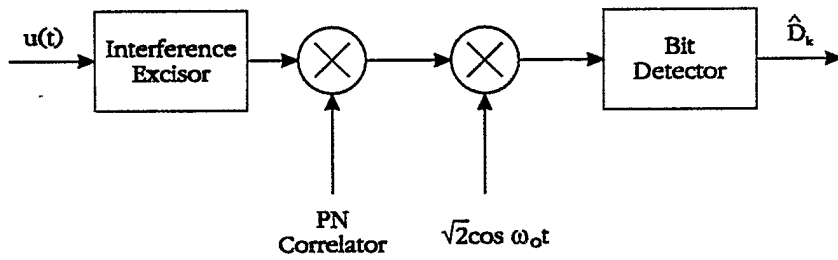
$$s(t) = a_I(t) \cos(\omega_0 t) - a_Q(t) \sin(\omega_0 t) \quad (2)$$

where $\omega_0 = 2\pi f_0$ and

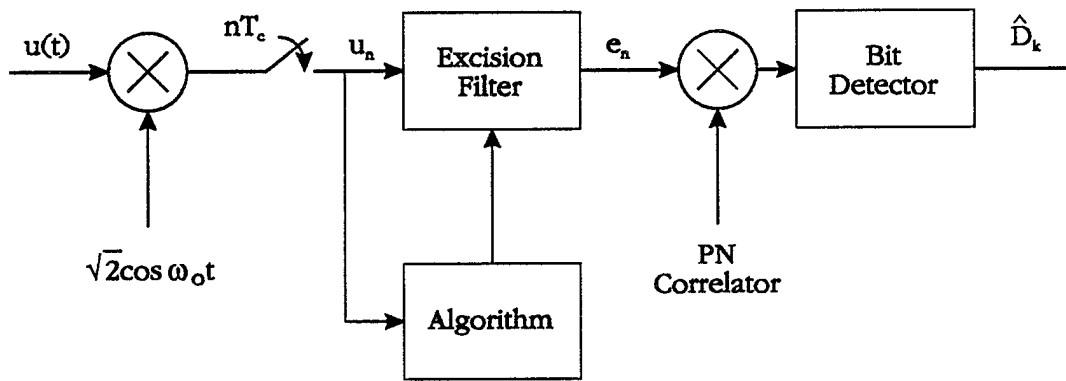
$$a_I(t) = \sum_k D_{I,k} b_{I,k}(t - kT_b) \quad (3)$$

and

$$a_Q(t) = \sum_k D_{Q,k} b_{Q,k}(t - kT_b). \quad (4)$$



(a)



(b)

Figure 2: Two conceptual approaches to interference excision for BPSK signals: (a) Analog excisor; (b) Digital excisor.

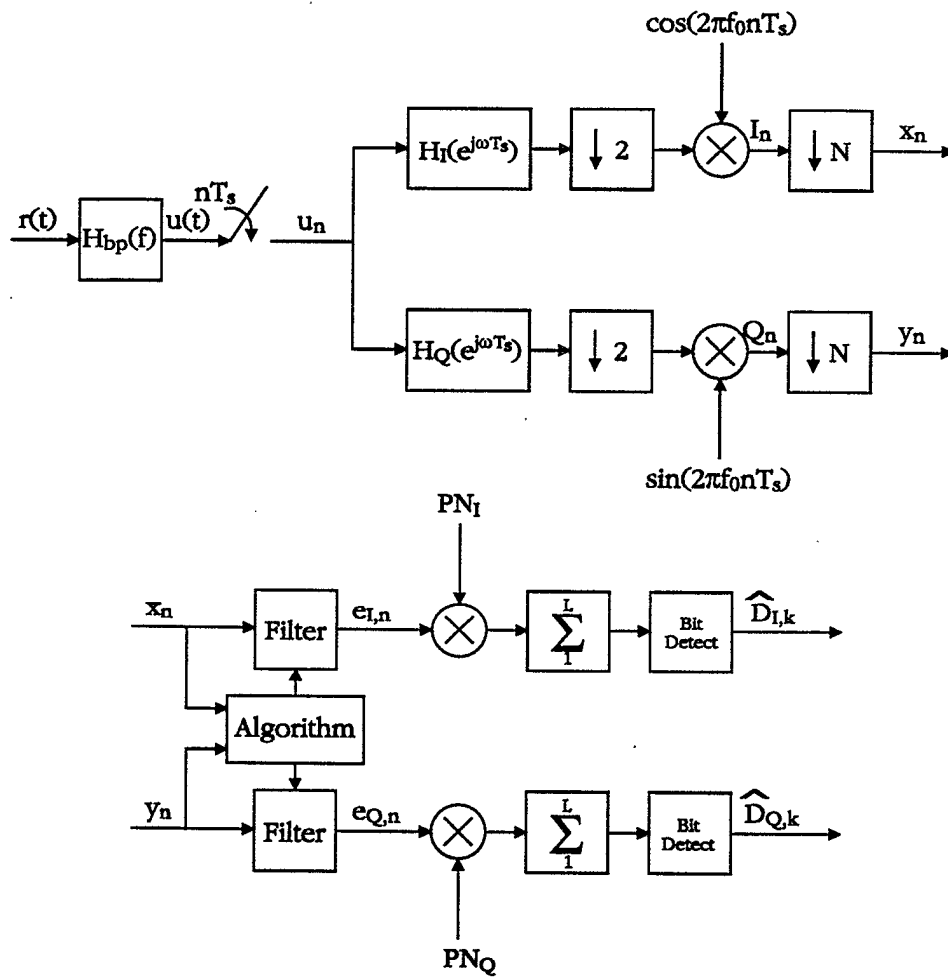


Figure 3: Spread spectrum communications model.

In Eqs. (3) and (4), $D_{I,k}$ and $D_{Q,k}$ are sequences of in-phase and quadrature data bits of duration T_b seconds, and $b_{I,k}(t - kT_b)$ and $b_{Q,k}(t - kT_b)$ are the in-phase and quadrature PN sequence patterns for the k^{th} bit, i.e.,

$$b_{I,k}(t) = \sum_{j=1}^L c_{I,kj} q(t - jT_c) \quad (5)$$

$$b_{Q,k}(t) = \sum_{j=1}^L c_{Q,kj} q(t - jT_c) \quad (6)$$

with L being the number of pseudo random chips per bit, or the processing gain, $c_{I,kj}$ and $c_{Q,kj}$ are the code sequences for the bits, and $q(t)$ represents the basic chip pulse of energy E_c .

The noise $n(t)$ is Gaussian and has a power spectral density

$$S_n(f) = \frac{N_0}{2} |H_{bp}(f)|^2, \quad (7)$$

where $N_0/2$ is the power spectral density of the assumed white Gaussian noise from the channel.

The interference is a tone and is defined as

$$i(t) = A \cos(\omega_i t + \theta), \quad (8)$$

where A is the amplitude of the interference, $\omega_i = 2\pi f_i$ is the angular frequency of the interference offset from the spread spectrum frequency ω_0 by $\delta\omega = 2\pi\delta f$, and θ is a random phase with a value taken from a uniform probability density distribution from $-\pi$ to π radians.

Referring to Fig. 3, the output $u(t)$ of the bandpass filter is bandpass sampled at $f_s = 2B_{bp}$ where the relation $mf_s = f_0 + B_{bp}/2$ holds and m is an integer equal to $f_0/2B_{bp} + 1/4$. This relationship results in the digital domain spectrum illustrated in Fig. 4 in which the noise samples are uncorrelated and the spread spectrum signal has been filtered to $B_{bp} = NR_c$ where, in this example, $N = 8$. The resultant sampled signal is, therefore,

$$u_n = s_n + n_n + i_n, \quad (9)$$

where s_n is the sampled spread spectrum signal, n_n are uncorrelated noise samples, and i_n are correlated interference samples. The digitized signal u_n is applied to two digital bandpass filters H_I and H_Q in quadrature with one another and of bandwidth less than

B_{bp} . The outputs of these digital filters are decimated by 2 and digitally mixed down to baseband,⁴ the result of which are the in-phase and quadrature digital signals I_n and Q_n which are further decimated by a factor N to the chip rate. The resulting decimated signals $\{x_n, y_n\}$ are applied to the adaptive filter whose coefficients are calculated by the algorithm described in the next section.

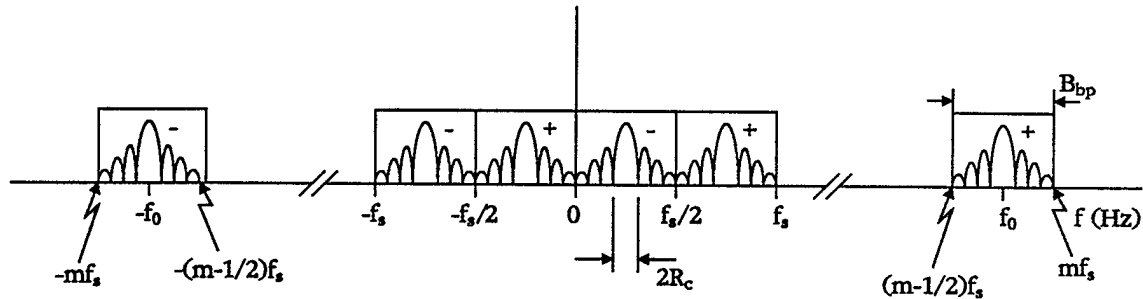


Figure 4: Sampled spread spectrum signal and noise at the output of the analog bandpass filter H_{bp} of bandwidth B_{bp} .

4.0 EXCISION FILTER ALGORITHM

This section will describe the FFT-based suppression algorithm as outlined in [2, 10].

The basis for the FFT method is that the power density spectrum of the spread spectrum signal is relatively flat while the spectrum of the narrow-band interference is highly peaked. This is particularly true for the sampled signal $\{x_n, y_n\}$ at the output of the decimator in Fig. 3. There, each signal sample (chip) can be viewed as being independent of other signal samples, resulting in a “white-noise” signal sequence, whereas each interference sample, because of its narrowband nature, is highly correlated with past and future interference samples.

The first step in this method is to estimate the power spectral density of the signals $\{x_n, y_n\}$. The spectral estimate can be obtained by the Welch method [12], where the in-phase and quadrature channels can be combined to form the complex signal $z_n = x_n + j y_n$ from which the power spectrum can be determined.

Once the PSD of the received signal is estimated for a given block of data, the interference suppression filter can be designed for that block. A transversal filter is an appropriate structure for this application, since it is desired to use a filter that contains

⁴The carrier frequency as represented by the RF source to be discussed later in Fig. 5 was accurately adjusted to 0.001 Hz so as not to produce crosstalk between the in-phase and quadrature channels for the duration of an experiment.

notches (zeroes) in the frequency range occupied by the interference. A method for designing the transversal filter in the discrete-time domain is to select its discrete Fourier transform (DFT) to be the reciprocal of the square root of the power spectral density at equally spaced frequencies.

To elaborate, suppose that the transversal filter has K taps. Since it is not desired to have a notch at 0 or π radians, a Type 1 filter (K odd, and symmetric impulse response) will be required. The problem is to specify the set of K tap coefficients $\{h_n\}$ or equivalently its DFT defined as

$$H_k = \sum_{n=0}^{K-1} h_n e^{-j\frac{2\pi}{K}nk}, \quad k = 0, 1, \dots, K-1. \quad (10)$$

In terms of the PSD of the received signal, H_k is given by

$$H_k = \frac{1}{\sqrt{P(k/K)}} e^{-j\frac{2\pi}{K}(\frac{K-1}{2})k} \quad (11)$$

where $P(f)$, defined for $0 \leq f \leq 1$ Hz, denotes the estimate of the PSD. Note that $P(f)$ is periodic with period 1 Hz and the folding frequency is 1/2 Hz. For a linear phase filter, the impulse response h_n must be conjugate symmetric (i.e., $h_n = h_{K-1-n}^*$).

Since the FFT algorithm produces a spectrum consisting of an even number of values but an odd number of taps are required, an interpolation algorithm operating on the given PSD samples from the Welch algorithm must be carried out. For example, if a K -tap filter is desired ($K = 15$, say) and the power spectrum consists of $M = 16$ or 32 samples at frequencies 0 to $(M-1)/M$ Hz in steps of $1/M$ Hz, values for $P(k/K)$ in Eq. (11) would have to be obtained at equally spaced intervals over the range 0 to $(K-1)/K$ Hz in intervals of $1/K$ Hz. The steps taken to calculate a set of filter coefficients $\{h_n\}$ for the suppression filter are listed in Table 1.

After the block of data has been filtered, the outputs of the suppression filter, $e_{I,n}$ and $e_{Q,n}$ in Fig. 3, are applied to the PN correlators. It should be noted that, because of a group delay of $(K-1)/2$ samples caused by the suppression filter, the PN correlators must be delayed by this amount as well.

5.0 EXPERIMENTAL SET-UP

The experimental set-up is illustrated in Fig. 5 and consists of equipment to generate the spread spectrum signal, interference, and broadband noise. It also has a bandpass filter, a bandpass digitizer (DAR 4000), and digital processors (VMEC30's and SUN 4/470).

Table 1: Excision Filter Algorithm.

- (1) Acquire block of data
- (2) Calculate power spectrum $P(k/M)$, $k = 0, 1, \dots, (M - 1)$
- (3) Linear interpolate $P(k/M)$ at $k = 0, 1, \dots, (K - 1)$
- (4) Calculate $1/\sqrt{P(k/K)}$, $k = 0, 1, \dots, (K - 1)$
- (5) Calculate H_k from Eq. (11)
- (6) Calculate the filter coefficients h_n
- (7) Filter the block of data collected in step 1
- (8) Return to step one

Also included are reference clocks and frequency synthesizers and several attenuators to set up the desired signal, noise and interference levels.

The baseband spread spectrum signal was generated by a New Wave Instruments LRS 100 signal generator which has the capability of producing pseudo random data spread by a maximum length sequence PN code with a predefined period. The user also selects the desired processing gain and modulation type; BPSK modulation was chosen for these experiments. The chip rate can be controlled by an internal or an external clock. The baseband spread spectrum signal was applied to a PSK modulator whose output was the spread spectrum signal centered at frequency $f_0 = 21.875$ MHz. The parameters for the generation of the spread spectrum signal are listed in Table 2. The 21.875 MHz carrier, LRS 100 and DAR 4000 were all stabilized by a 10 MHz rubidium frequency standard.

The composite signal consisting of signal, noise and interference, shown in Fig. 5 entering a combiner, are applied to a bandpass filter centered at 21.875 MHz and of 10 dB bandwidth 6.25 MHz. Its output, after attenuation to a desired level, was fed to the DAR 4000 which digitized the analog input. The digitized signal was further filtered by linear phase FIR bandpass filters in quadrature with one another. The in-phase and quadrature outputs of these filters were decimated by a factor of 2 and mixed down to baseband; these

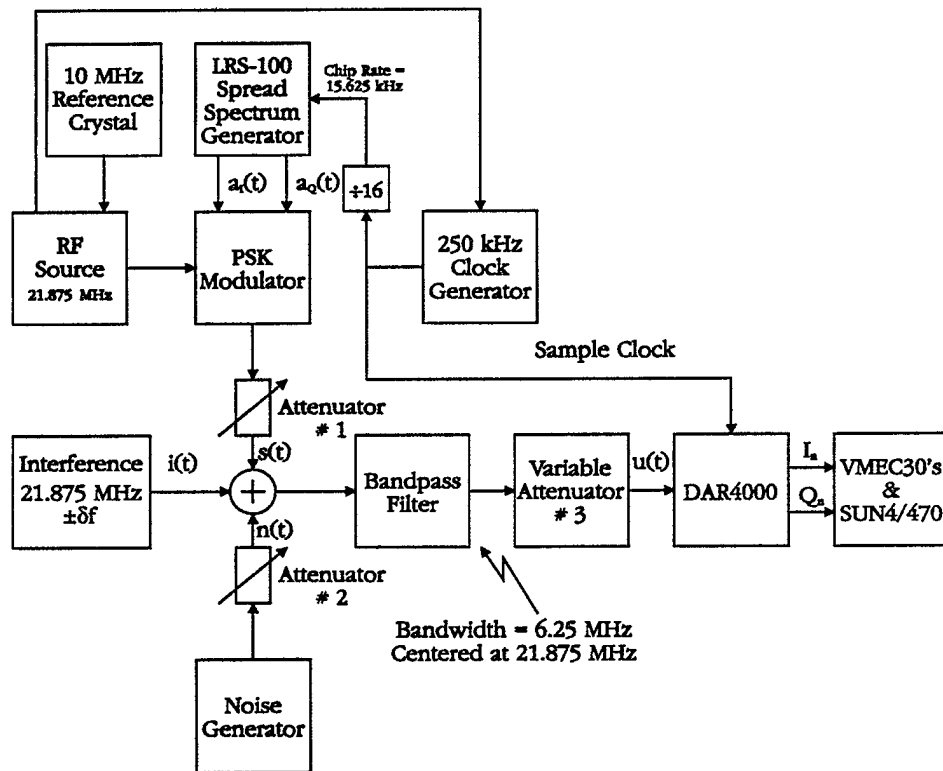


Figure 5: Experimental setup for excision experiments.

steps are shown in Fig 6. The parameters of the bandpass filters were set by the user to provide uncorrelated noise samples after the output of the DAR 4000 had been decimated to the chip rate R_c in the VMEC30 processors (this refers to the outputs $\{x_n, y_n\}$ in Fig. 3). For example, if the sampling rate at the output of the DAR 4000 was $8R_c = 125$ kHz, and the digital bandpass filters had bandwidths of 93.75 kHz, decimation by 8 will result in a valid sampling frequency to produce uncorrelated noise samples. This can be seen by noting that a lowpass filter with an ideal rectangular frequency response of two-sided bandwidth $2B$ and with white noise at its input, will result in a stochastic process at its output having an autocorrelation function with nulls at $n/2B$, $n = 1, 2, \dots$. The reciprocal of these terms corresponds to sampling frequencies which yield uncorrelated noise samples. In the above example, $B = 46.88$ kHz meets these requirements and is the value used in the experiments described next.

Table 2: Spread Spectrum Signal Parameters.

Parameter	Value
Bit rate, R_b	1.5625 kHz
Chip rate, R_c	15.625 kHz
Processing gain, L	10
Carrier frequency, f_0	21.875 MHz
Modulation	BPSK
Code length	15
PN cyclic pattern	{ -1 1 -1 -1 1 1 -1 1 1 1 -1 -1 -1 -1 1 }

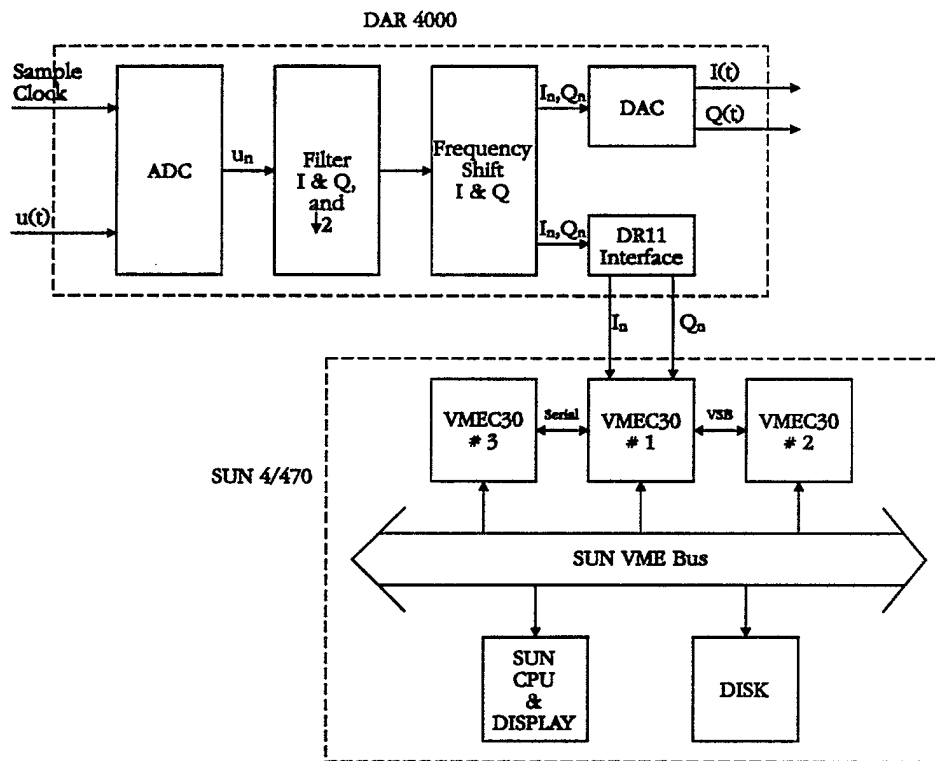


Figure 6: DAR 4000 and VMEC30 sub-systems of Fig. 5.

6.0 EXPERIMENTAL RESULTS

This section presents several of the experimental results based on the systems in Figs. 5 and 6.

Figure 7 illustrates several frames of the background system digital noise, obtained by not applying any signal, additive noise, nor interference into the front end of the DAR 4000 in Fig. 5. The amplitude level is the decimal equivalent of a signed 15-bit binary number. The power spectra of the system noise and system noise plus additive noise at the output of the DAR 4000 are illustrated in Fig. 8⁵. The purpose of this plot is to show the relative power levels of the two noises. The additive noise in this case was set at the minimum value used in the experiments. This plot was calculated using the Welch algorithm with a rectangular window. A block of 65,536 (64K) samples was collected and the power spectra were calculated on the basis of averaging 512 point sub-blocks with no overlapping.

Figure 9 illustrates the power spectra for both noises after decimation by a factor of 8 in the VMEC30 processors in Fig. 6. The power spectrum for the total noise (system plus additive) shows its "whiteness", which was expected given the filter parameters that were selected as discussed in the previous section. The total block size was 8192 points, with 512 points being the sub-block size and no overlapping.

Figure 10 illustrates several frames of the unspread data sequence. Observe that the system noise level for this example is significant relative to the data. The power spectrum of the unspread data is illustrated in Fig. 11

Figure 12 shows two frames of the PN sequence at the output of the DAR 4000 prior to decimation by 8 in the VMEC30 board; the plot shows a time-shifted version of the PN code in Table 2. The effect of system noise is quite evident (note that no additive noise was applied at the input). In fact, on the VMEC30 board where the decimation occurs, the centre sample of the chip was selected, which can result in a fluctuation from chip sample to chip sample of in the order of 2 to 6 dB. This would produce a degradation in the bit error rate results compared to the case when ideal data is used. Figure 13 illustrates what the situation would have been like had the data in Fig. 12 been applied to a digital version of an integrate-and-dump system which is a matched filter for rectangular chips. The effect of this filtering would have been to suppress some of the

⁵It should be understood that ten times the logarithm of the linear power spectral values (relative to a single unit) at each of the frequencies has been taken. Thus, to obtain the total power, one would have to convert the dB values back to linear values and then sum the power contribution of each frequency component. Also, the abscissa has been normalized to 1 Hz by dividing by the sampling rate $f_s = 125$ kHz.

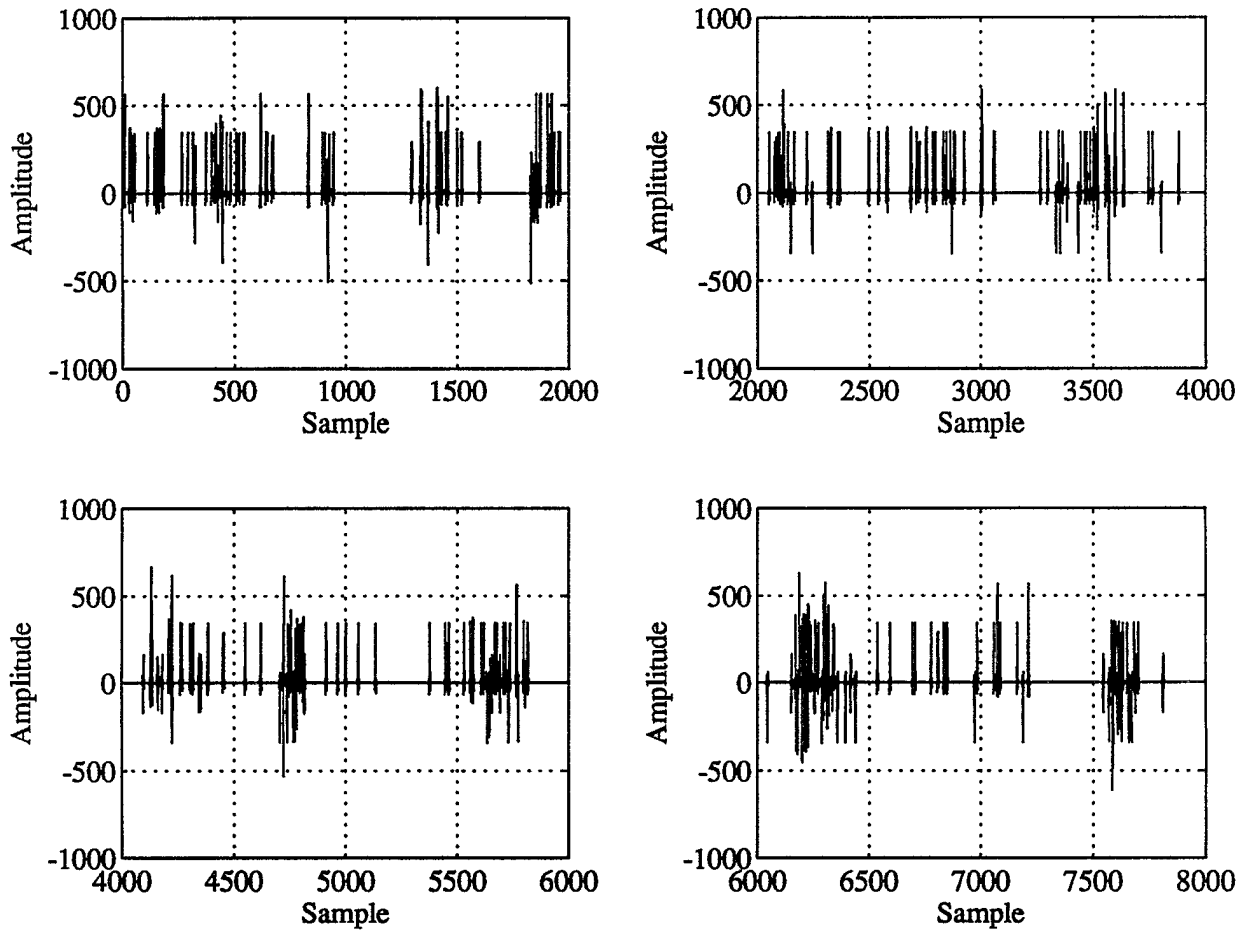


Figure 7: Several frames of system digital noise at the output of the DAR 4000.

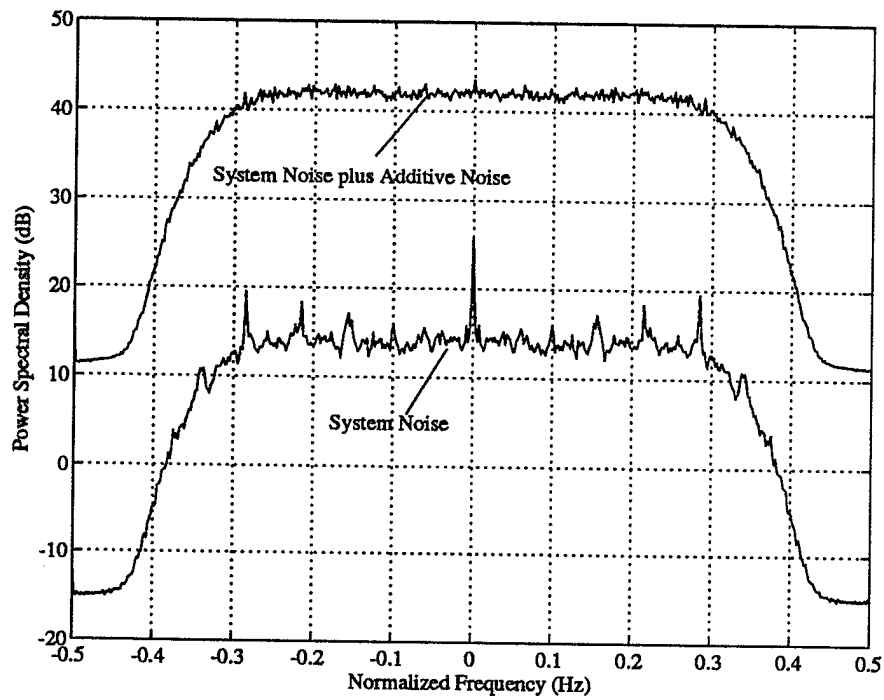


Figure 8: Power spectral densities of system noise and additive noise plus system noise before decimation; the abscissa has been normalized by $f_s = 125$ kHz.

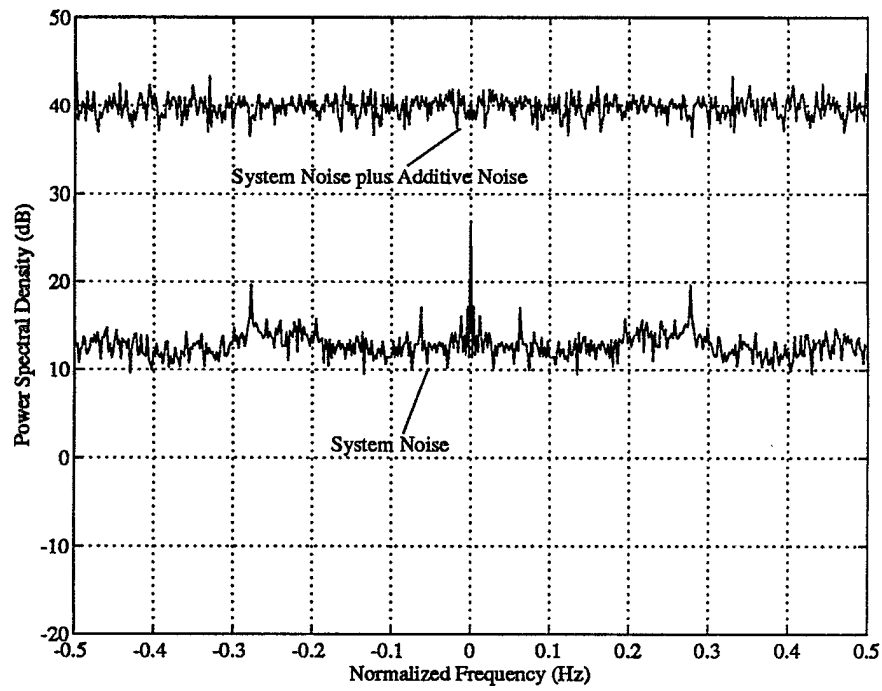


Figure 9: Power spectral densities of system noise and additive noise plus system noise after decimation.

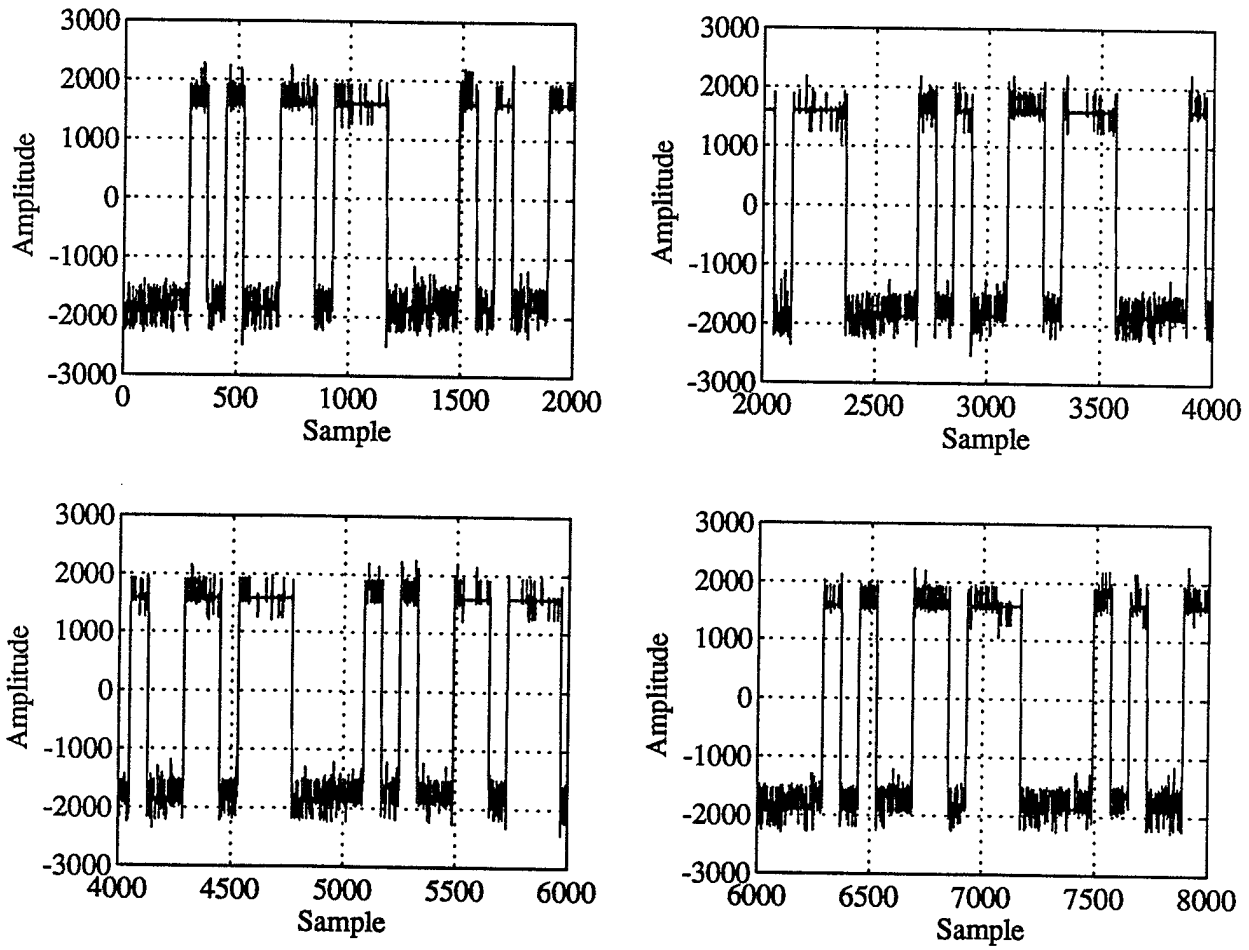


Figure 10: Several frames of the unspread data sequence at the output of the DAR 4000. The number of samples per bit is 80 (i.e., 8 samples/chip).

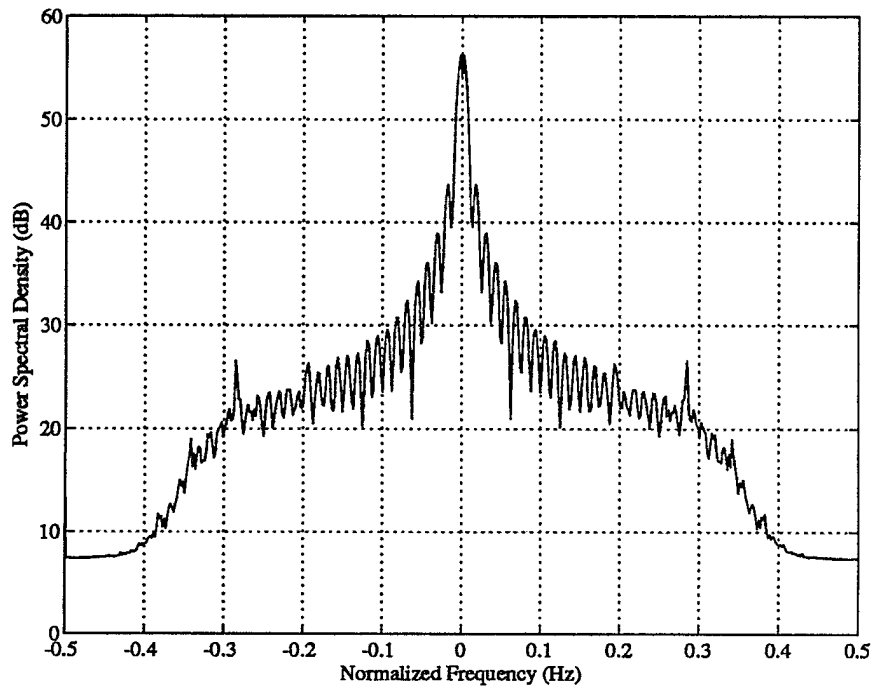


Figure 11: Power spectral density of unsread data sequence at the output of the DAR 4000.

system noise as seen by the apparent decrease in the fluctuation. This approach, however, was not implemented in the VMEC30's.

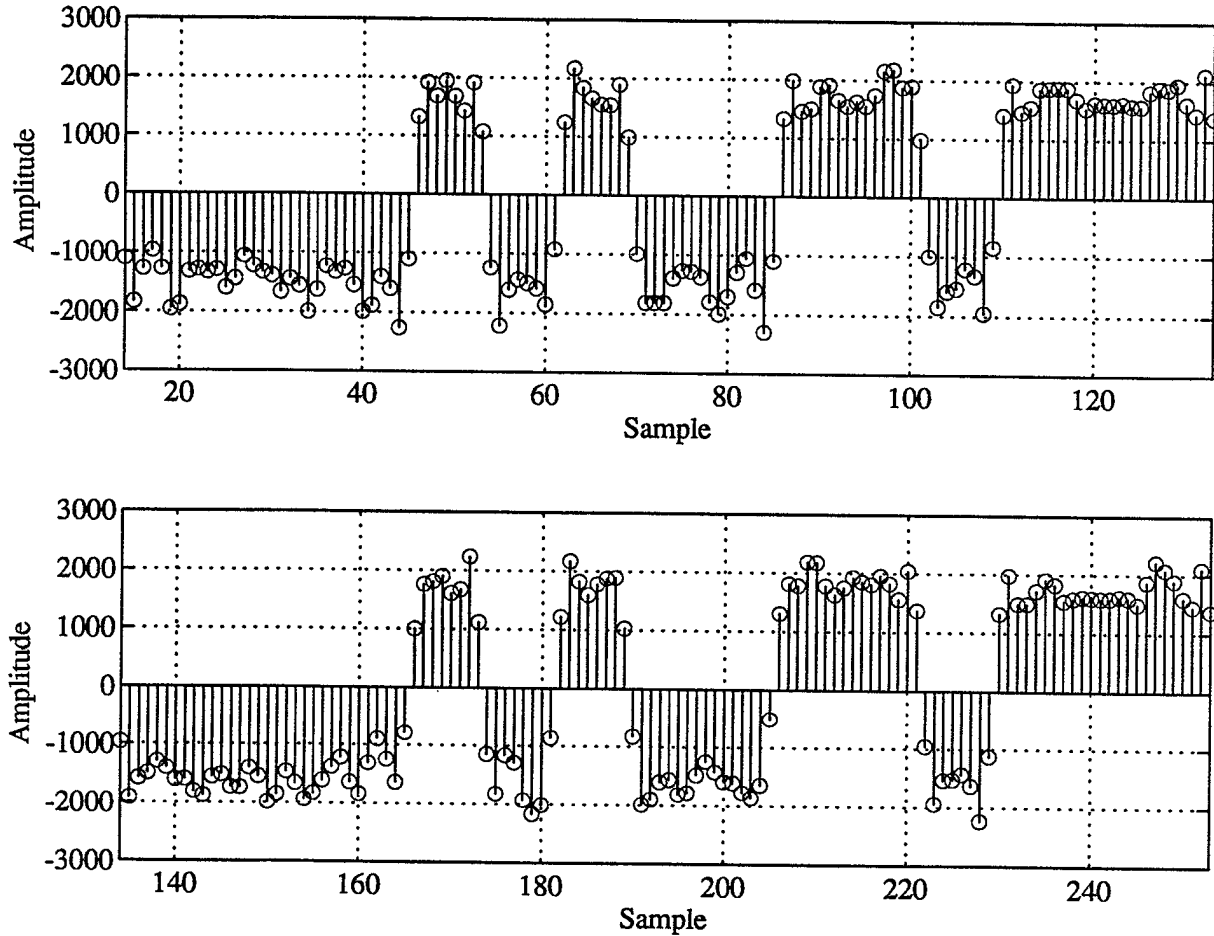


Figure 12: Two frames of the PN sequence at the output of the DAR 4000 with a sampling rate of 8 samples/chip.

The power spectra of the PN sequence and the spread signal are illustrated in Figs. 14 and 15. The Welch algorithm was used with an overall block size of 64K samples where the sub-block size was 512 points; the window was rectangular. Figure 14 shows the distinct spectral lines of the spreading sequence. Notice too that the bandwidth of the DAR 4000 had been set up to be about $6R_c$ (93.75 kHz). For the spread signal in Fig. 15, the distinct lines have disappeared since the resolution used was not sufficient to

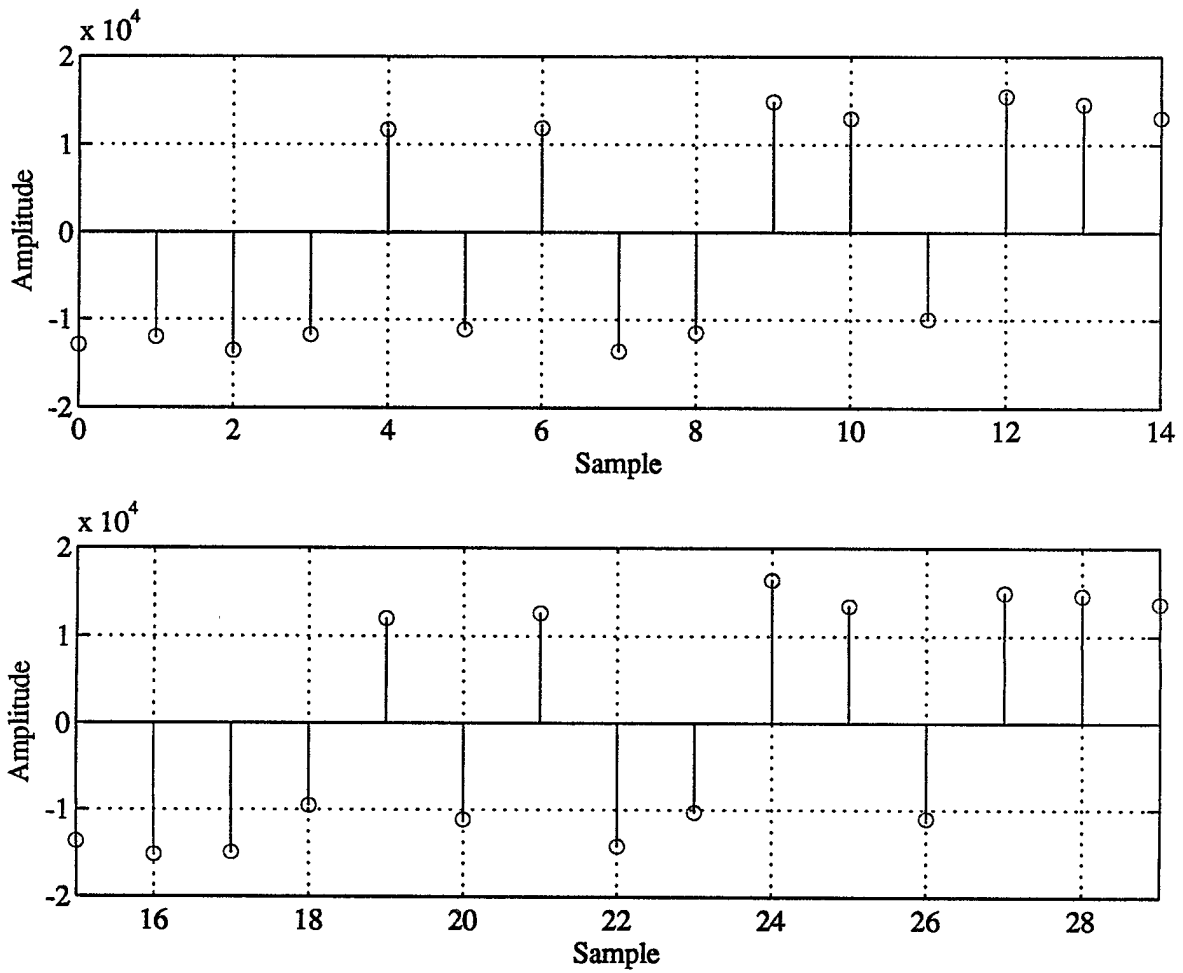


Figure 13: What the two frames of the PN sequence code in Fig. 12 would look like if they had been applied to a digital version of an integrate-and-dump system operating at the chip rate.

show them.⁶

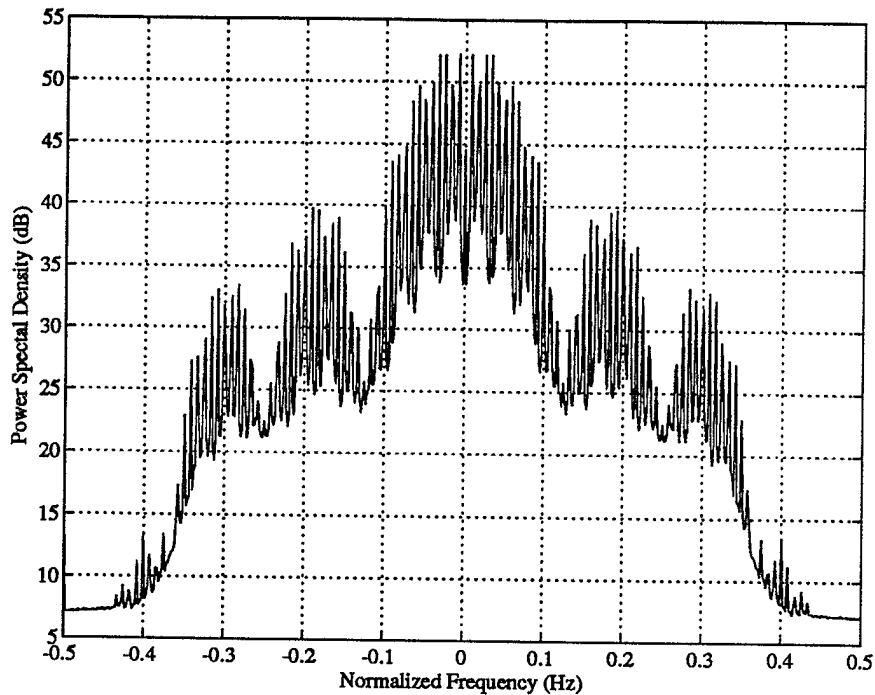


Figure 14: Power spectral density of a block of samples of the spreading sequence at the output of the DAR 4000.

Figure 16 illustrates an example of interference and system noise in the time and frequency domains. The frequency offset was 3 kHz (i.e., $0.024f_s$) from the spread spectrum carrier. Figure 17 shows examples of the time and frequency domain data for the case when $E_b/N_0 = 5$ dB and the interference-to-signal ratio was equal to 20 dB. Figure 18 illustrates the power spectrum for the case in which the interference-to-signal ratio was 10 dB and the interference was offset from the carrier by 10 Hz and 3 kHz.

As noted earlier, the output of the DAR 4000 is applied to one of the VMEC30 processors via the DR11 interface (see Fig. 6). There, the data is decimated by a factor of 8 in this case, and the resultant data is used to calculate the desired filter coefficients. Figure 19 shows an example of the power spectrum of the decimated data. It can be seen that the background “noise” is “white”, whereas the interference is quite evident. The decimated data are the input to the estimation algorithm described in Section 4.0, where

⁶Had a higher resolution FFT been used, distinct lines would have appeared since pseudo-random data instead of random data was used.

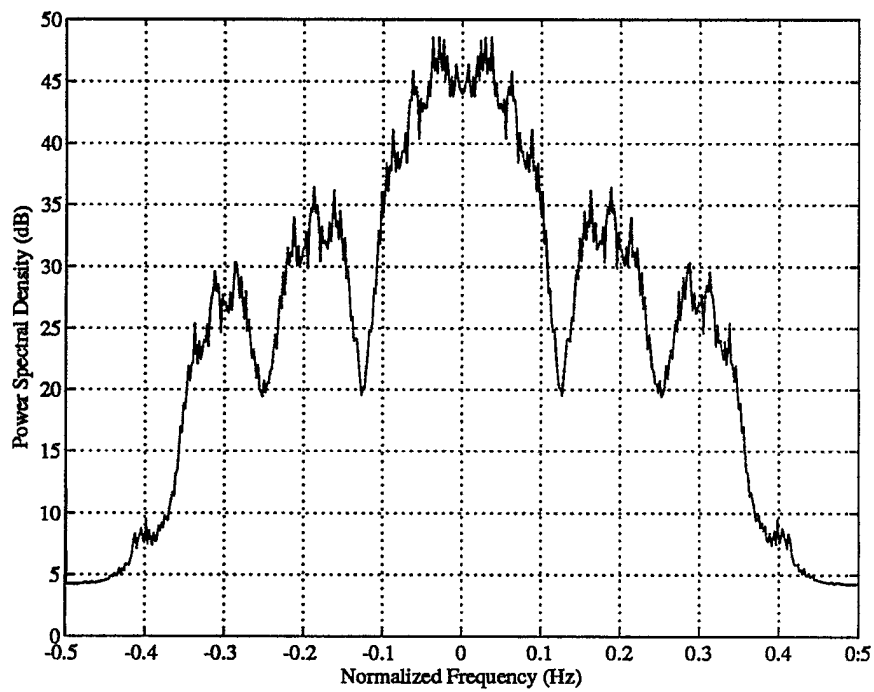


Figure 15: Power spectral density of a block of samples of the spread spectrum signal at the output of the DAR 4000.

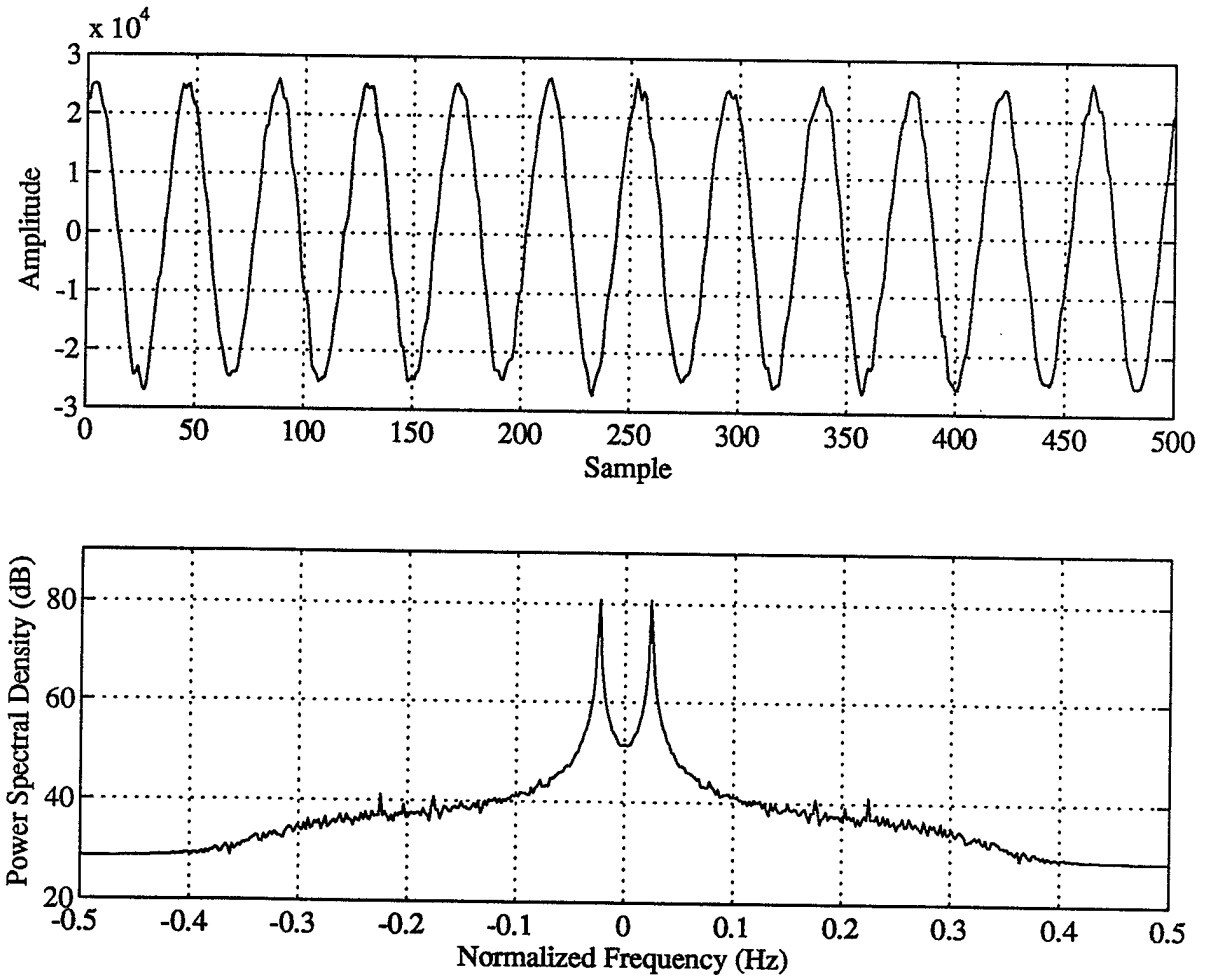


Figure 16: An example of the tone interference (located at 0.024 Hz) plus system noise in the time domain (upper frame) and frequency domain (lower frame) at the output of the DAR 4000.

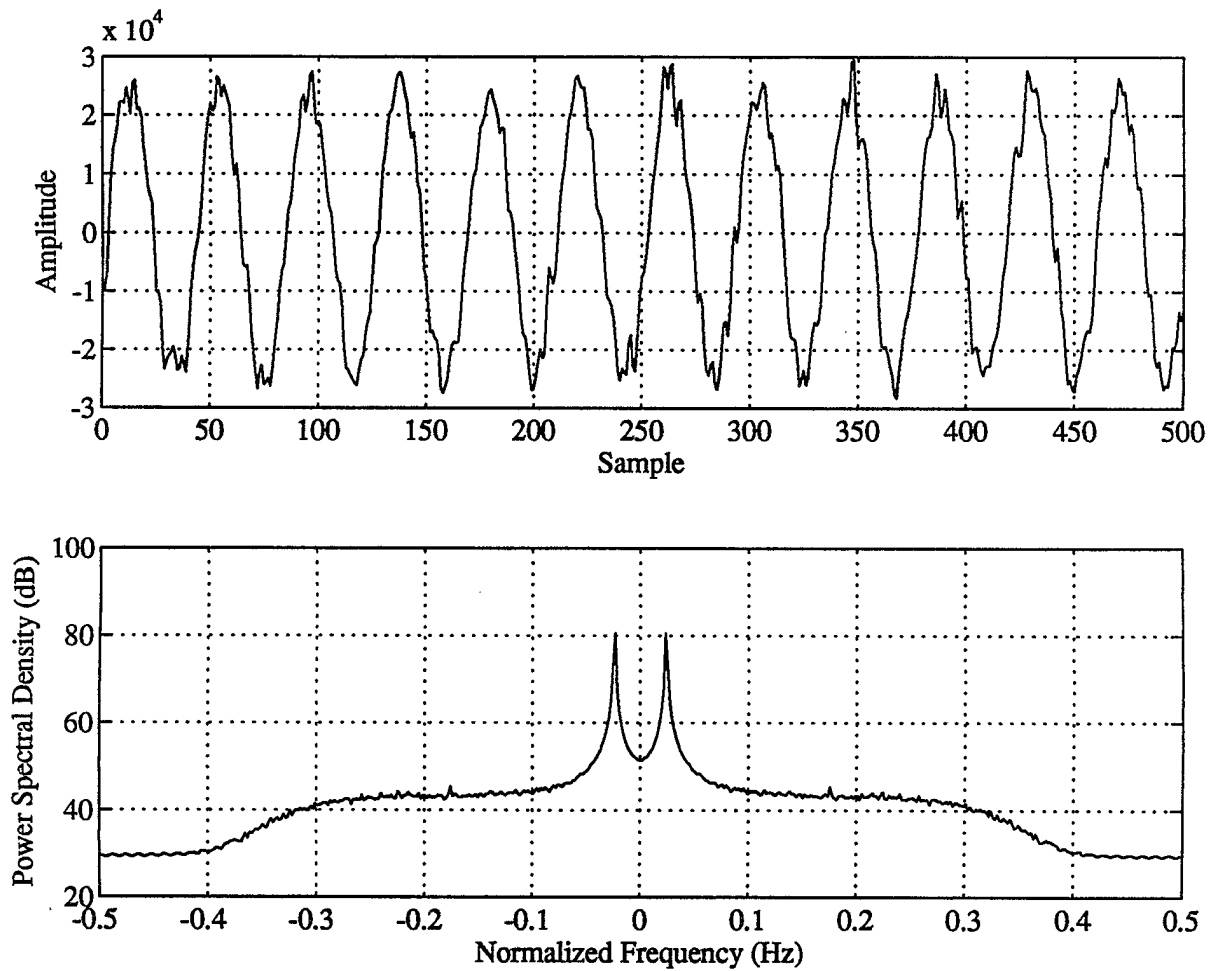


Figure 17: Signal, noise and tone interference (located at 0.024 Hz) in the time domain (upper frame) and frequency domain (lower frame) at the output of the DAR 4000; $E_b/N_0 = 5$ dB, interference-to-signal ratio equal to 20 dB.

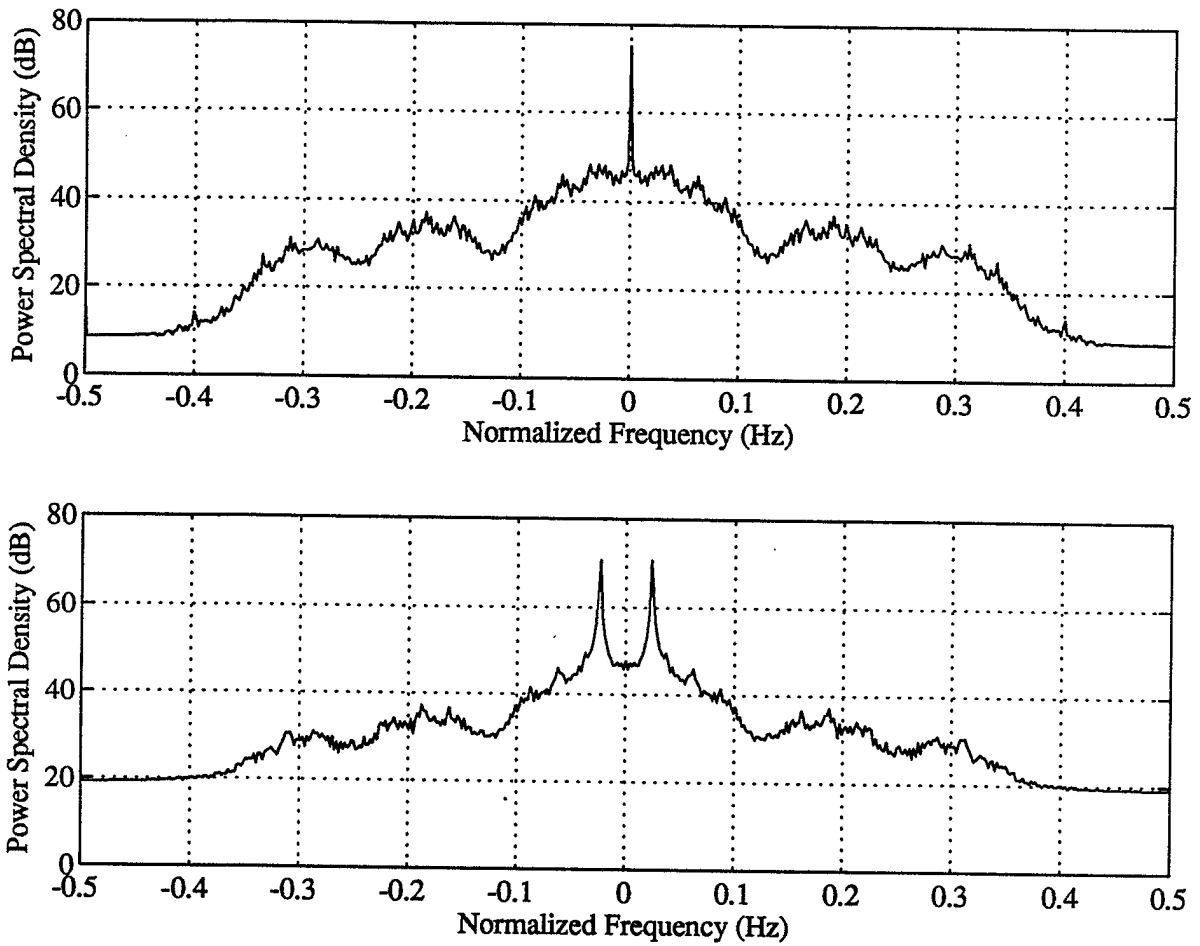


Figure 18: Power spectra of signal plus tone interference located at 8×10^{-5} Hz (upper frame) and 0.024 Hz (lower frame) at the output of the DAR 4000; interference-to-signal ratio equal to 10 dB. Additive noise was not present.

the coefficients of the excision filter are calculated.

Several snapshots of the frequency response of the excision filters based on successive blocks of data are shown in Fig. 20. Each frequency response was calculated from a block size of 512 points and sub-block size of 32 points. The filter order was 31. Examples of the power spectra of the input and output of the notch filter are illustrated in Fig. 21. For this example the attenuation of the tone is approximately 30 dB.

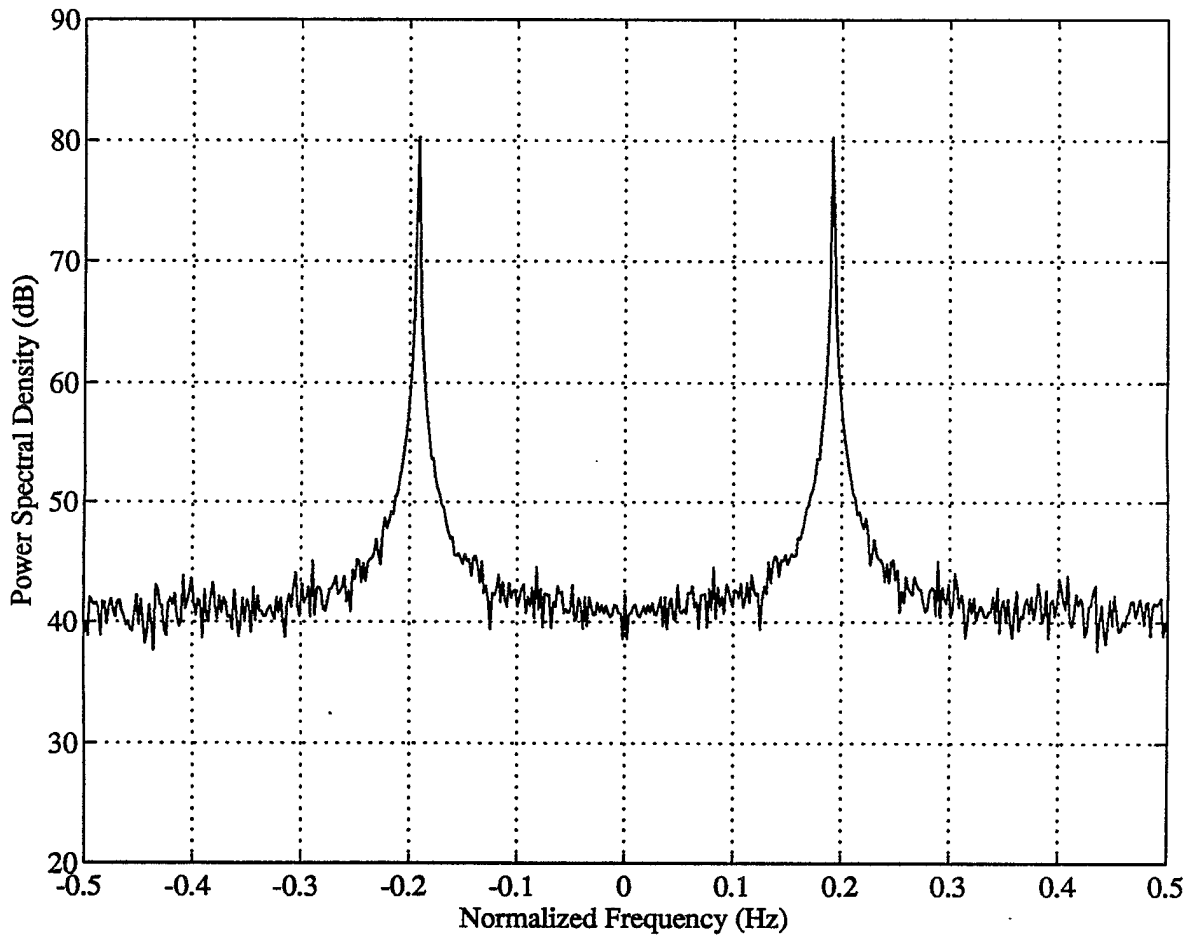


Figure 19: Power spectrum of signal, noise and tone interference (located at 0.024 Hz) in the time domain after decimation by 8 in the VMEC30 board; $E_b/N_0 = 5$ dB, interference-to-signal ratio equal to 20 dB.

Figure 22 illustrates the bit error rate of experimental and theoretical data without the excisor. The theoretical bit error rate curve for BPSK signals in additive white

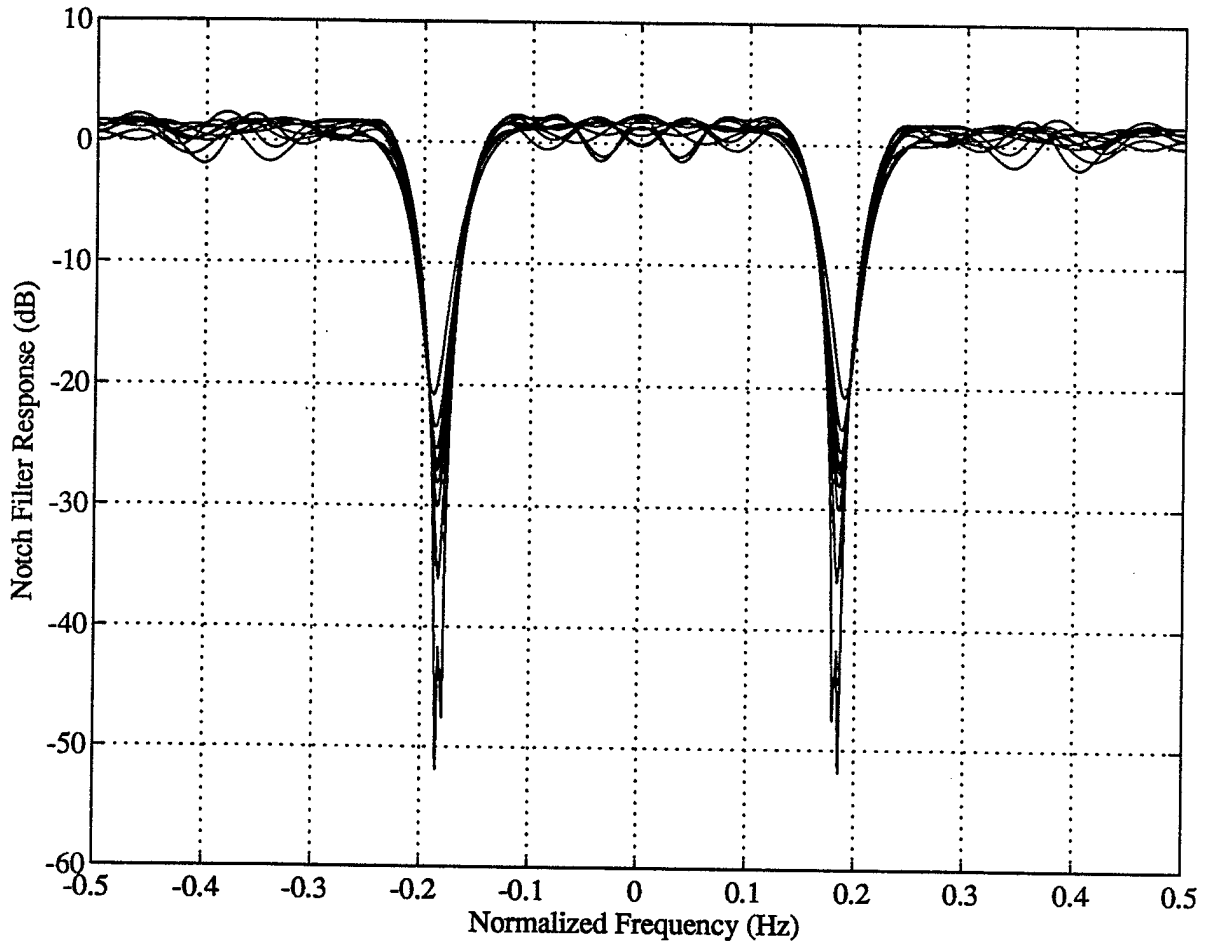


Figure 20: Several notch filter frequency responses as calculated by the VMEC30 processor based on a tone with system noise only (no additive noise). Each frequency response curve was calculated from a block size of 512 and subblock size of 32. The filter order was 31, the sampling rate was decimated by a factor of 8 (i.e., $125/8 = 15.625$ kHz), and the tone frequency was located at 3 kHz (normalized frequency of 0.192 Hz).

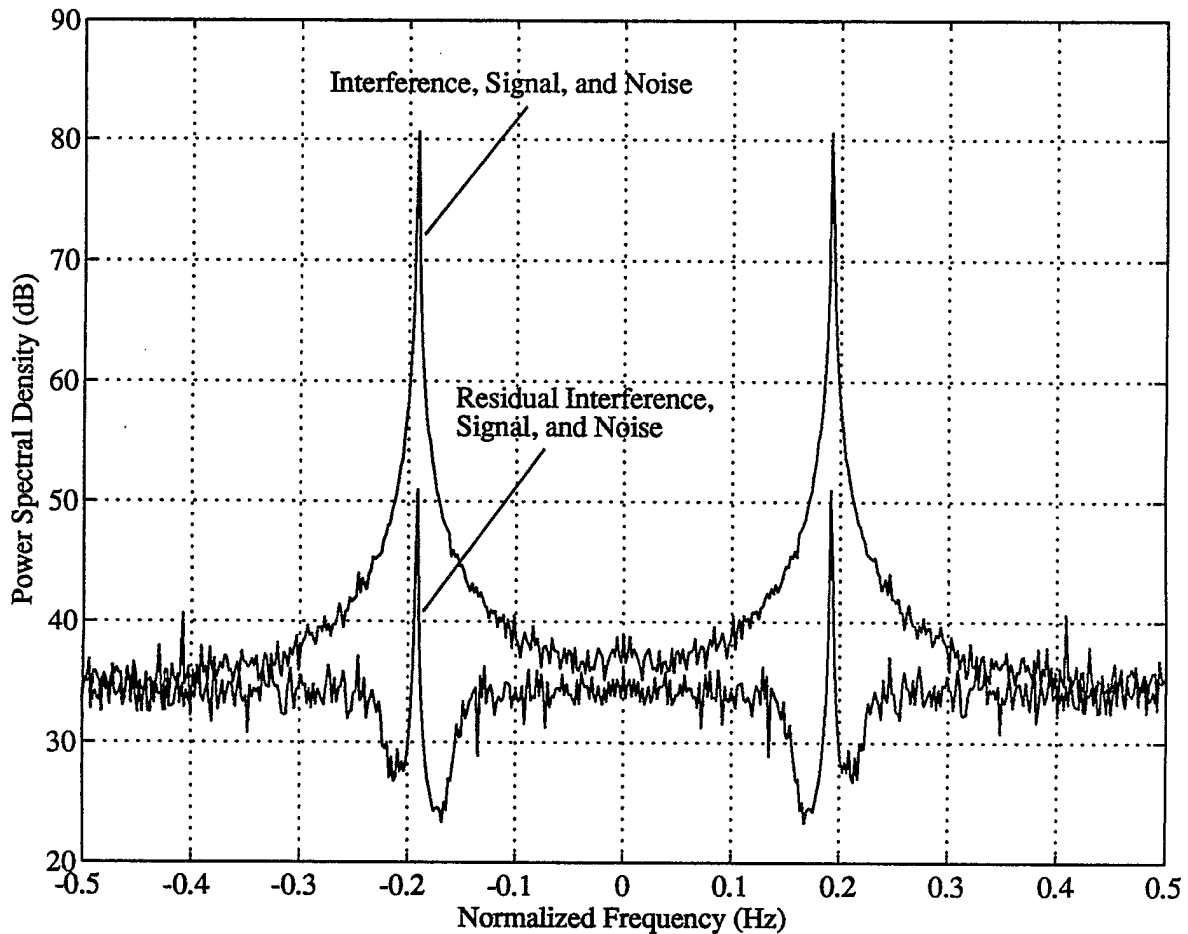


Figure 21: Effect of the excision filter. The two power spectra shown were each calculated from a block of 8192 points using the Welch algorithm, with sub-blocks of 512 points, no overlapping, and a rectangular window. The excision filter coefficients were calculated from block sizes of 512 points and sub-block sizes of 32 points. The filter order was 31, the sampling rate was decimated by a factor of 8 (i.e., $125/8 = 15.625$ kHz), and the tone frequency was located at 3 kHz (normalized frequency of 0.192 Hz).

Gaussian noise is defined as

$$P_b = \frac{1}{2} \operatorname{erfc}(\sqrt{E_b/N_0}). \quad (12)$$

where E_b is the energy per bit, N_0 is the single-sided noise power spectral density, and erfc is the complementary error function. As can be seen, the experimental results are approximately within 0.2 dB of theory. Given experimental error and the effect of system noise on each chip, this would seem to be reasonable. It should be noted that signal-to-noise ratios were calculated on the basis of a 64K block of decimated data. This was accomplished by first collecting a block of only system noise and determining its power. Once this power was calculated it was removed from the total power obtained from a block of signal plus system noise. This was similarly done to determine the power contribution of the additive noise. Finally, in determining the experimental bit error rate curve, 15 million chip samples (1.5 million bits, since the processing gain L was 10) were stored on disk and then correlated with the PN code, the results of which were bit detected.

Figure 23 illustrates the performance with and without the excision filter present⁷. The interference-to-signal ratio was 10 dB and the interference was offset from the carrier of the spread spectrum signal first by 10 Hz and then by 3 kHz. As can be seen from the results, when the filter was not present, the bit error rate was approximately 0.35. With the filter present, the performance improves somewhat. How much it improves depends on the location of the tone relative to the carrier. As was pointed out in [13], the performance is a function of the location of the tone relative to the carrier. Finally, the results for the case when the interference-to-signal ratio was set at 20 dB are illustrated in Fig. 24. Under these conditions, the performance has degraded somewhat compared with the results in Fig. 23.

7.0 CONCLUSIONS

This technical note has presented the experimental results of a proof-of-concept of an FFT excision system using a digitizer and three TMS320C30 processors.

With interference present, the results showed that an improvement in performance of the spread spectrum system can be achieved when the excisor is functioning, although the algorithm employed is not optimum in the sense that a mean-squared-error function is not being minimized. It would be interesting to compare the performance of the FFT approach to the Widrow-Hoff LMS algorithm and the block and/or recursive least squares algorithms.

⁷It should be noted that decimation to the chip rate followed by excision were done in real time, whereas PN correlation and bit detection were done off line.

The performance of the FFT approach is a function of the FFT size and the window. Further investigation of these parameters is required and will be the subject of further studies. Contributing to the variation in performance of the excision technique was the relatively high system noise produced by the DAR 4000. It was suggested that by incorporating a digital filter matched to a chip, and sampling the output of this matched filter at the chip rate would filter out some of this noise.

One of the laborious aspects of implementing this algorithm (and perhaps any others to be implemented in ACES at a later date) was determining a balanced distribution of the workload across the three TMS320C30 processors. Efficient ways of reducing the development/testing cycle will have to be incorporated into the ACES system when attempting to implement algorithms for any application. Even with the effort that was required to implement the excision application, the overall bandwidth of the spread spectrum signal had to be scaled down significantly so as to implement a real-time interference suppression capability. It should be noted too that even with scaling down the frequencies of operation, the despreading had to be done off-line.

The next step will be to implement the FFT and other techniques in a system having a higher quality digital receiver and other processors, thus allowing for an increase in the bandwidth of operation. In fact, the system being considered for this will utilize a Steinbrecher receiver, Austek FFT processors and a 9 cell iWarp array.

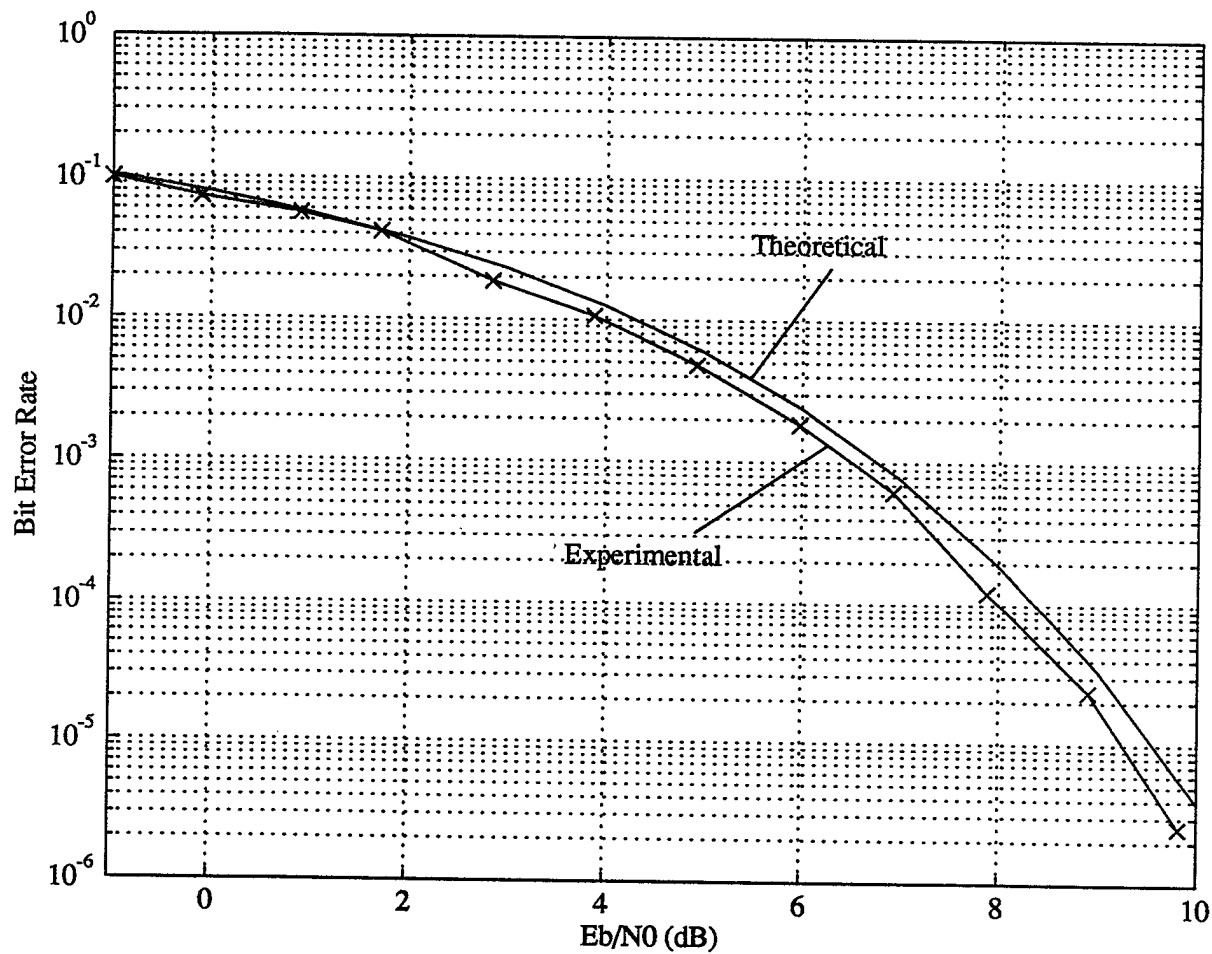


Figure 22: Theoretical and experimental bit error rate curves based on signal-to-noise ratios calculated at the output of the DAR 4000. No interference was present.

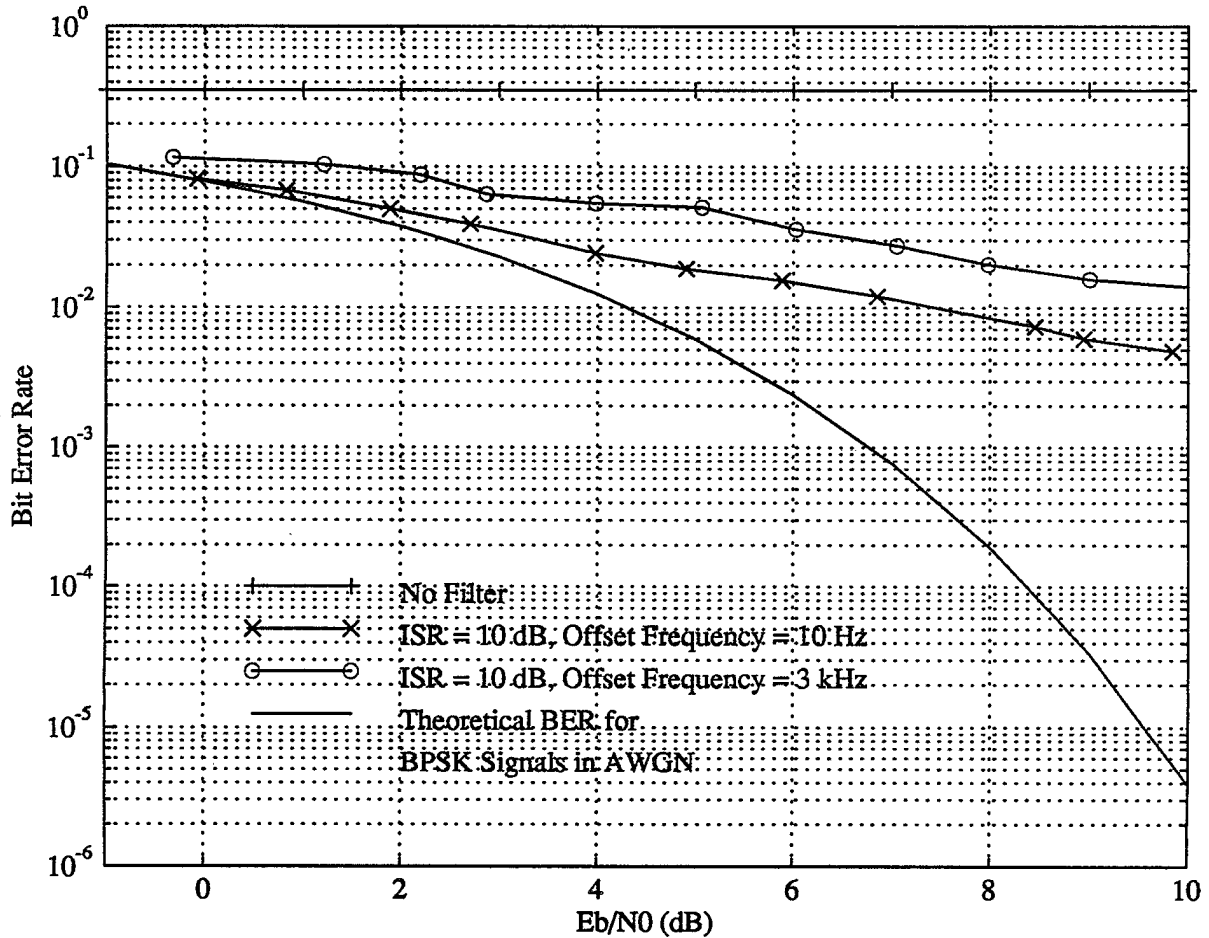


Figure 23: Theoretical and experimental bit error rate curves for single-tone interference located at frequencies f_i of 10 Hz and 3 kHz offset from the carrier. The signal-to-noise and interference-to-signal ratios were calculated at the output of the DAR 4000.

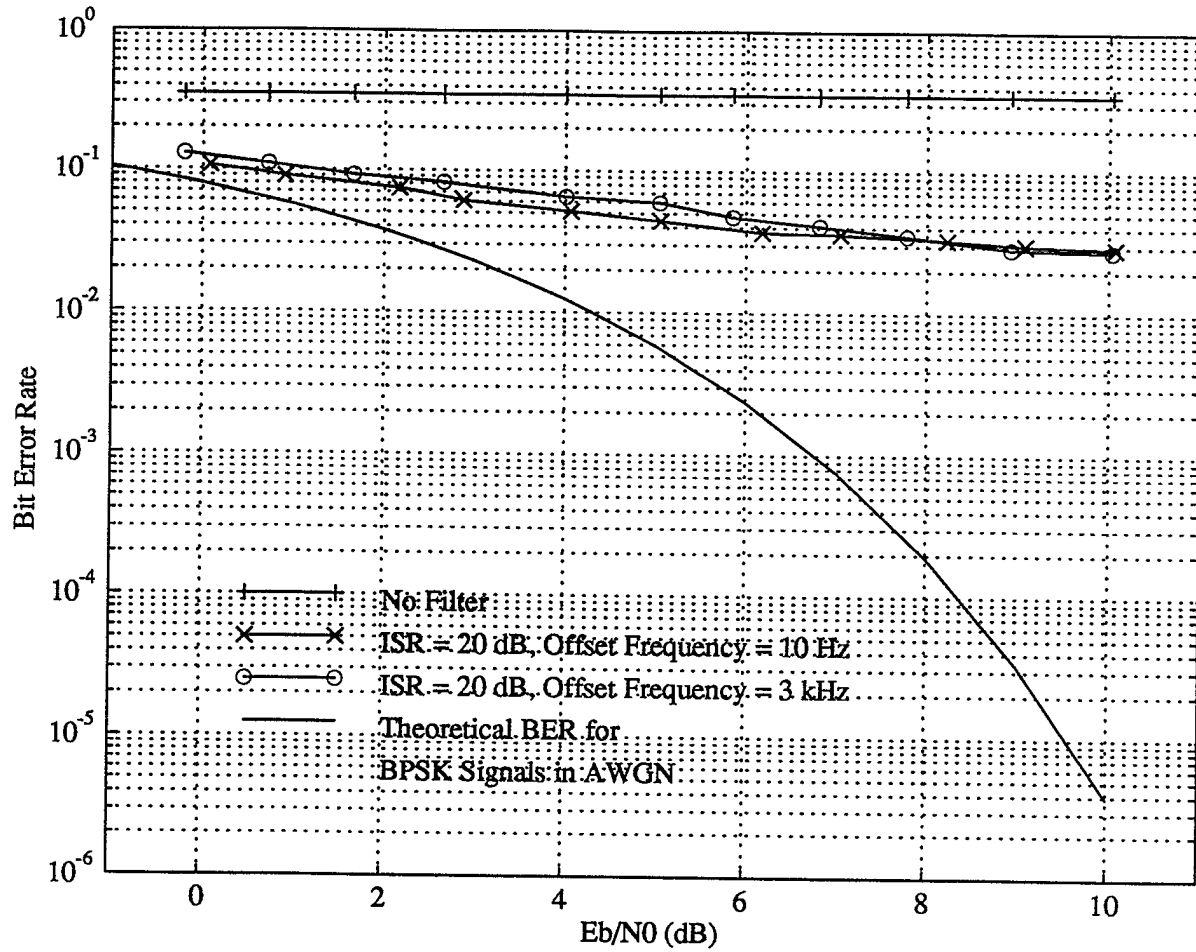


Figure 24: Theoretical and experimental bit error rate curves for single-tone interference located at frequencies f_i of 10 Hz and 3 kHz offset from the carrier. The signal-to-noise and interference-to-signal ratios were calculated at the output of the DAR 4000.

REFERENCES

- [1] F. M. Hsu and A. A. Giordano, "Digital whitening techniques for improving spread spectrum communications performance in the presence of narrowband jamming and interference," *IEEE Transactions on Communications*, vol. 26, pp. 209–216, February 1978.
- [2] J. W. Ketchum and J. G. Proakis, "Adaptive algorithms for estimating and suppressing narrowband interference in PN spread-spectrum systems," *IEEE Transactions on Communications*, vol. 30, pp. 913–924, May 1982.
- [3] L. B. Milstein, "Interference rejection techniques in spread spectrum communications," *Proceedings of the IEEE*, vol. 76, pp. 657–671, June 1988.
- [4] B. W. Kozminchuk, "Kalman filter-based architectures for interference excision," Technical Report 1118, Defence Research Establishment Ottawa, Ottawa, Ontario, Canada, K1A 0Z4, 1991.
- [5] B. W. Kozminchuk, "A comparison of recursive least squares and Kalman filtering excisors for swept tone interference," Technical Note 92-14, Defence Research Establishment Ottawa, Ottawa, Ontario, Canada, K1A 0Z4, 1992.
- [6] J. P. Burg, "Maximum entropy spectrum analysis," in *Modern Spectrum Analysis* (D. G. Childers, ed.), pp. 34–41, New York: IEEE Press, 1978.
- [7] B. Widrow, J. M. McCool, M. G. Larimore, and C. R. Johnson, "Stationary and nonstationary learning characteristics of the LMS adaptive filter," *Proceedings of the IEEE*, vol. 64, pp. 1151–1161, August 1976.
- [8] S. L. Marple, "A new autoregressive spectrum analysis algorithm," *IEEE Transactions on Acoustics, Speech, and Signal Processing*, vol. 28, pp. 441–454, August 1980.
- [9] J. M. Cioffi and T. Kailath, "Fast, recursive-least-squares transversal filters for adaptive filtering," *IEEE Transactions on Acoustics, Speech, and Signal Processing*, vol. 32, pp. 304–337, April 1984.
- [10] B. W. Kozminchuk, "A Fast Fourier Transform approach to interference suppression in direct sequence spread spectrum signals," Technical Note 93-2, Defence Research Establishment Ottawa, Ottawa, Ontario, Canada, K1A 0Z4, 1992.

REFERENCES

- [11] D. Elsaesser and B. W. Kozminchuk, "Advanced communications ESM system (ACES) design considerations," Technical Note 92-2, Defence Research Establishment Ottawa, Ottawa, Ontario, Canada, K1A 0Z4, 1992.
- [12] F. J. Harris, "On the use of windows for harmonic analysis with the discrete Fourier transform," *Proceedings of the IEEE*, vol. 66, pp. 51-83, January 1978.
- [13] L. Li and L. B. Milstein, "Rejection of narrowband interference in PN spread-spectrum systems using transversal filters," *IEEE Transactions on Communications*, vol. 30, pp. 925-928, May 1982.

13. ABSTRACT (a brief and factual summary of the document. It may also appear elsewhere in the body of the document itself. It is highly desirable that the abstract of classified documents be unclassified. Each paragraph of the abstract shall begin with an indication of the security classification of the information in the paragraph (unless the document itself is unclassified) represented as (S), (C), or (U). It is not necessary to include here abstracts in both official languages unless the text is bilingual).

(U) An FFT-based algorithm for suppressing narrowband interference in direct sequence spread spectrum signals has been implemented across three TMS320C30 processors forming part of the Advanced Communications Electronic Support Measures System (ACES). An FFT approach is especially attractive because of its computational economy. The basic problem to be solved is described, following by a description of the algorithm. This technique is feasible so long as the bandwidth of the interference during the observation time over which the FFT is calculated is much less than the bandwidth of the spread spectrum signal. One of the laborious aspects of implementing this algorithm (and perhaps any others to be implemented on ACES at a later date) was to efficiently distribute the workload across the three TMS320C30 processors so as to achieve real-time performance; this objective was achieved, although the spread spectrum bandwidths which could be processed were not high. The experience gained will demand the incorporation of efficient ways of reducing the development/testing cycle in the ACES system when attempting to implement algorithms for any signal processing application.

14. KEYWORDS, DESCRIPTORS or IDENTIFIERS (technically meaningful terms or short phrases that characterize a document and could be helpful in cataloguing the document. They should be selected so that no security classification is required. Identifiers, such as equipment model designation, trade name, military project code name, geographic location may also be included. If possible keywords should be selected from a published thesaurus. e.g. Thesaurus of Engineering and Scientific Terms (TEST) and that thesaurus-identified. If it is not possible to select indexing terms which are Unclassified, the classification of each should be indicated as with the title.)

INTERFERENCE
SUPPRESSION
SPREAD SPECTRUM
EXCISION
ADAPTIVE FILTERING
FOURIER TRANSFORM

13. ABSTRACT (a brief and factual summary of the document. It may also appear elsewhere in the body of the document itself. It is highly desirable that the abstract of classified documents be unclassified. Each paragraph of the abstract shall begin with an indication of the security classification of the information in the paragraph (unless the document itself is unclassified) represented as (S), (C), or (U). It is not necessary to include here abstracts in both official languages unless the text is bilingual).

(U) An FFT-based algorithm for suppressing narrowband interference in direct sequence spread spectrum signals has been implemented across three TMS320C30 processors forming part of the Advanced Communications Electronic Support Measures System (ACES). An FFT approach is especially attractive because of its computational economy. The basic problem to be solved is described, following by a description of the algorithm. This technique is feasible so long as the bandwidth of the interference during the observation time over which the FFT is calculated is much less than the bandwidth of the spread spectrum signal. One of the laborious aspects of implementing this algorithm (and perhaps any others to be implemented on ACES at a later date) was to efficiently distribute the workload across the three TMS320C30 processors so as to achieve real-time performance; this objective was achieved, although the spread spectrum bandwidths which could be processed were not high. The experience gained will demand the incorporation of efficient ways of reducing the development/testing cycle in the ACES system when attempting to implement algorithms for any signal processing application.

14. KEYWORDS, DESCRIPTORS or IDENTIFIERS (technically meaningful terms or short phrases that characterize a document and could be helpful in cataloguing the document. They should be selected so that no security classification is required. Identifiers, such as equipment model designation, trade name, military project code name, geographic location may also be included. If possible keywords should be selected from a published thesaurus. e.g. Thesaurus of Engineering and Scientific Terms (TEST) and that thesaurus-identified. If it is not possible to select indexing terms which are Unclassified, the classification of each should be indicated as with the title.)

INTERFERENCE
SUPPRESSION
SPREAD SPECTRUM
EXCISION
ADAPTIVE FILTERING
FOURIER TRANSFORM

#143924

NO. OF COPIES NOMBRE DE COPIES	COPY NO. COPIE N°	INFORMATION SCIENTIST'S INITIALS INITIALES DE L'AGENT D'INFORMATION SCIENTIFIQUE
1	1	JL
AQUISITION ROUTE FOURNI PAR	DREO	
DATE	18 Jul 94	
DSIS ACCESSION NO. NUMÉRO DSIS	95-00104	

DND 1168 (6-87)



PLEASE RETURN THIS DOCUMENT TO THE FOLLOWING ADDRESS:
 DIRECTOR
 SCIENTIFIC INFORMATION SERVICES
 NATIONAL DEFENCE
 HEADQUARTERS
 OTTAWA, ONT. - CANADA K1A 0K2

PRIÈRE DE RETOURNER CE DOCUMENT À L'ADRESSE SUIVANTE:
 DIRECTEUR
 SERVICES D'INFORMATION SCIENTIFIQUES
 QUARTIER GÉNÉRAL
 DE LA DÉFENSE NATIONALE
 OTTAWA, ONT. - CANADA K1A 0K2